UNIVERSIDADE DE LISBOA

FACULDADE DE CIÊNCIAS

DEPARTAMENTO DE QUÍMICA E BIOQUÍMICA

Characterization of *cdkn2b* gene during zebrafish development

Cátia Alexandra Vieira Crespo

DISSERTAÇÃO

MESTRADO EM BIOQUÍMICA

2012

UNIVERSIDADE DE LISBOA

FACULDADE DE CIÊNCIAS

DEPARTAMENTO DE QUÍMICA E BIOQUÍMICA

Characterization of *cdkn2b* gene during zebrafish development

Cátia Alexandra Vieira Crespo

Dissertation supervisors:

External supervisor: Dra. Patrícia Abrantes
Internal supervisor: Dra. Carla Real Afonso

DISSERTAÇÃO
MESTRADO EM BIOQUÍMICA

2012

Acknowledgements

It is a pleasure to thank the many people who made this thesis possible.

I would like to express my gratitude to my supervisor António Jacinto. Thanks for giving me the opportunity to be part of your lab, making my master project such an enriching experience. Special thanks to my supervisor, Dra. Patrícia Abrantes, whose expertise, understanding, and patience, added considerably to my experience.

To Professor Carla Afonso thanks for being my internal supervisor.

I would also like to thank all members of Tissue Repair Unit for their help and patience, especially to Rita Mateus, Mariana Simões, Fábio Valério, Inês Cristo, Ana Cristina. To Ângela Dias for her companionship, patience, and company in all weekends we stayed on the lab.

To Lara Carvalho and Aida Barros for their indispensable help, patience, support and company in all the hours I have passed in the fish facility. Thank you also for all the advise and putting up with all my crazy cross schedule and music, especially in this last period.

To José Rino and António for their teaching and help with all bioimaging equipment that I needed.

To UDEV Unit and Vânia from UNIC for their advise and help when I needed.

To Pedro Silva for his patience and precious help in the statistical work of my thesis.

I also wish to express my gratitude to Audrey Lopes for her support, company and friendship. For making me laugh and all the patience hearing me talk about all my experiments during lunch time.

To all my friends especially to: Inês Andrade, Elisabete Ribeiro, João Fernandes, João Amorim, João Vieira, Duarte Azevedo, Ana Sousa, André Gomes and Ana Santos for their friendship, support, for putting up with me in times of stress, and for their patience hearing me talk about zebrafish all the time. Without you I wouldn´t have such a full life.

Finally, I would like to thank my family for the support they provided me through my entire life and for creating a loving environment for me. Especially to my father, Ricardo Crespo and mother, Julieta Crespo, that given me the opportunity of making this master.

Abbreviations

ANRIL: antisense non-coding RNA in the INK4 locus

BA: basilar artery

CAD: coronary artery disease

CaDI: caudal division of the internal carotid artery

CDKs*:* cyclin-dependent kinases

CDKIs: cyclin-dependent kinase inhibitors

cv: caudal vein

DA: dorsal aorta

DLAV: dorsal longitudinal anastomotic vessel

dpf: days post-fertilization

EBL: epidermal basal layer

EVL: enveloping layer

GFP: green fluorescent protein

GWAS: genome-wide association studies

hpf: hours post-fertilization

IA: intracranial aneurysm

min: minutes

ml: milliliter

mM: milimolar

Mo: antisense morpholino oligonucleotide

mRNA: messenger Ribonucleic Acid

ng: nanograms

PBS: phosphate buffered saline

PCV: posterior (caudal) cardinal vein

PICA: primitive internal carotid artery

pRB: retinoblastoma protein

SAH: subarachnoid hemorrhage

Se: intersegmental vessel

SeA: intersegmental artery

SeV: Intersegmental vein

SIA: supraintestinal artery

SIV: subintestinal veins

SNP: single-nucleotide polymorphisms

TGFβ: transforming trowth factor β

wt: wild type

Resumo

CDKN2B (inibidor de quinase dependente de ciclina 2B), também conhecido como *INK4b* ou *p15*^{INK4b}, é um dos membros da família INK4 (CDK inibidores) e, é conhecido pelo seu papel em processos de proliferação celular, envelhecimento, e função como supressor de tumores. Nos seres humanos, o *CDKN2B* está numa região em que foi identificado um novo locus associado com o risco de desenvolver aneurismas intracranianos (locus 9p21) em diferentes populações europeias e na população japonesa. Aneurisma intracraniano ocorre da dilatação de um vaso sanguíneo causada por doença ou enfraquecimento da parede do vaso.

Apesar dos recentes avanços das técnicas moleculares, os mecanismos de iniciação dos aneurismas intracranianos, progressão e rutura dos mesmos ainda são mal compreendidos, bem como o possível papel do locus 9p21 para os mecanismos subjacentes de aneurismas intracranianos não é conhecido.

Com o objetivo de superar a complexidade da etiologia genética humana e, de perceber o possível envolvimento deste locus na formação de aneurismas intracranianos, fomos estudar um ortólogo do gene *CDKN2B* (*cdkn2b*) no peixe-zebra, um modelo animal muito atrativo para estudar vertebrados. O peixe-zebra possui uma combinação de vantagens que o tornam um modelo ideal. Além de ser um vertebrado, e, portanto, mais perto do humano do que os modelos de invertebrados, o peixe-zebra tem elevada fecundidade (algumas centenas de ovos por desova), os embriões são transparentes e desenvolvem-se externamente. Ao contrário dos em*b*riões de muitos outros vertebrados, os embriões são acessíveis à observação e manipulação em todas as fases do seu desenvolvimento e, possuem um tempo de gestação curto (2-3meses até serem adultos). Além disso, os peixe-zebra adultos também podem ser facilmente visualizados e manipulados experimentalmente. Para além de todas estas vantagens do modelo do peixe-zebra para o estudo do desenvolvimento em vertebrados, este também é um bom modelo para o estudo da biologia vascular. Isto deve-se à existência de uma linha transgénica de peixes-zebra (*fli1a:EGFP*) que contem um repórter (GFP) associado aos vasos sanguíneos, possibilitando assim a observação dos vasos durante todo o desenvolvimento do embrião.

Como as informações sobre o gene *cdkn2b* no peixe-zebra são escassas, começámos por proceder à sua caracterização durante os primeiros estadios de desenvolvimento (24, 48 e 72 horas pós fertilização [hpf]) em peixes-zebra AB *wt*. Para isso utilizámos técnicas de hibridação *in situ* para caracterizar a expressão de mRNA do *cdkn2b* e, de imunohistoquímica na caracterização da expressão proteica. Em seguida, de forma a tentar perceber qual a função

do gene, fizemos o *knockdown* do mesmo através da injeção de morfolinos, uma técnica muito utilizada nos dias de hoje para o knockdown de genes em peixes-zebra.

Dado que um dos objetivos deste projeto era ainda estudar a possível relação entre o *cdkn2b* e a formação dos vasos sanguíneos durante o desenvolvimento do peixe-zebra, o *knowkdown* do *cdkn2b* através da injeção de morfolinos, foi feito não só em AB *wt*, mas também em peixe-zebra *fli1a:EGFP.*

Começámos a caracterização do *cdkn2b* através do estudo da expressão do mRNA em AB *wt*. Em todos os *time-points* analisados (24, 48 e 72 horas pós fecundação), o *cdkn2b* apresentou expressão sobretudo na cabeça dos embriões. Mais especificamente, às 24hpf foi visível expressão no cérebro e na mesoderme da cabeça do peixe. Relativamente às 48hpf e 72hpf apenas podemos concluir que é expresso na cabeça do peixe, no entanto não é possível saber a sua localização exata.

Além da expressão de mRNA do *cdkn2b*, também é importante caracterizar a expressão da proteína. Por observação dos resultados, concluímos que existe expressão generalizada ao nível da epiderme do peixe, especialmente no citoplasma das células. A presença da proteína no citoplasma é consistente com os dados disponíveis desta proteína em peixe-zebra adultos.

A camada superficial da epiderme dos peixes é formada por queratinócitos. A partir de estudo *in vitro* de queratinócitos humanos e no murganho verificou-se que o aumento de TGF-β leva ao aumento do *CDKN2B*. Uma vez que o *CDKN2B* é um inibidor das ciclinas CDK4 e CDK6 levando à estagnação da célula na fase G1 do ciclo celular, acreditamos que o *cdkn2b* pode também ter um papel importante na regulação do ciclo celular na epiderme dos embriões do peixe-zebra. Mais especificamente na estagnação dos queratinócitos existentes na epiderme.

Curiosamente, às 48hpf e às 72hpf detetámos a presença de "lacunas de marcação" na epiderme, formando um padrão peculiar de expressão do *cdkn2b*. A camada mais externa da epiderme do embrião é formado por células vivas, queratinócitos, que não são renovados periodicamente, mas sim substituídas individualmente após a morte celular. Neste sentido, acreditamos que este padrão irregular (a presença das "lacunas de marcação") da expressão do *cdkn2b* pode dever-se à morte de células na epiderme do embrião e que ainda não tinham sido renovadas aquando o momento da fixação.

O facto de termos detetado expressão proteica do cdkn2b na epiderme do embrião não é contraditório com os resultados obtidos na hibridação *in situ*, tendo em conta que a deteção da expressão de mRNA pode ser insuficiente. Para esclarecer este ponto será necessário fazer hibridação *in situ* em secções do embrião.

Após a caracterização do *cdkn2b* fomos tentar estudar a função desta proteína no desenvolvimento embrionário. Para isso, decidiu usar-se morfolinos. Após a otimização das quantidades de morfolino a usar concluiu-se que, na ausência de *cdkn2b*, o fenótipo mais marcante é a curvatura para baixo do eixo do embrião e deformações ao nível da cauda. Embora os embriões tenham sido analisados às 24, 48 e 72hpf, a presença de fenótipo era mais marcante apenas a partir das 48hpf.

Após a utilização de um segundo morfolino contra o nosso gene de interesse, a realização de diversos controlos (injecção com morfolino standard, injecção com H_2O, co-injecção com o p53 Mo, injecção com p53 Mo) a confirmação do *knockdown* por imunohistoquímica e, o resgate do fenótipo, aquando da injeção de mRNA de *cdkn2b*, acreditamos ter fortes evidências da especificidade do fenótipo observado.

Em relação à possível relação entre *cdkn2b* e a formação de vasos sanguíneos, fizemos um *knockdown* em peixes-zebra transgénicos (*fli1a: EGFP*). Isso permitiu-nos analisar os vasos do peixe em detalhe nos estádios de desenvolvimento escolhidos.

Às 24hpf, o *knockdown* do *cdkn2b* promoveu a deformação da veia caudal assim como em fases posteriores do desenvolvimento embrionário (48hpf e 72hpf). No entanto, permanece a questão se os fenótipos observados na veia caudal são consequência de uma cauda deformada, ou se o *cdkn2b* está a afetar diretamente a formação do vaso, podendo levar a um fornecimento de sangue deficiente, provocando as deformações observadas durante o desenvolvimento da cauda do peixe.

Em conclusão, em embriões de peixes-zebra AB *wt* o *cdkn2b* é transcrito principalmente na cabeça do embrião. Ao nível das proteínas, há uma maior expressão na epiderme. Ao injetar um morfolino alvo para bloquear a tradução do *cdkn2b*, os embriões apresentam uma curvatura do eixo do embrião para baixo e, deformações ao nível da cauda. Isto demonstra a importância deste gene na correta formação do eixo e da cauda do peixe. Quanto aos vasos sanguíneos, são observadas alterações morfológicas ao nível da veia caudal dos transgénicos *fli1a: EGFP*, aquando do *knockdown* do *cdkn2b*. No entanto, serão necessários estudos complementares para entender a relação direta entre o *cdkn2b* e a formação do eixo do embrião, ou a formação da cauda e dos vasos da cauda.

Palavras-Chave: Peixe-zebra, embriões, *cdkn2b*, desenvolvimento, aneurismas.

Abstract

Cyclin-dependent kinase inhibitor 2B (*CDKN2B*), is known for its role in cell aging, proliferation, and function as a tumor suppressor. In humans, *CDKN2B* is in a region where a new risk locus associated with intracranial aneurysms was identified.

In order to overcome the complexity of human genetic etiology and to study the possible involvement of this locus in aneurysms formation, we have studied an ortholog (*cdkn2b*) of this gene in the zebrafish, a very attractive model system to study vertebrates. Since there is little information about this gene in zebrafish, we started by characterizing the gene during development of wild-type fish using *in situ* hybridization and immunohistochemistry techniques. We also did knock-down experiments by injecting morpholinos in *fli1a:EGFP* zebrafish, a transgenic that has the blood vessels marked with GFP.

The gene is transcribed mainly in the cephalic region of the fish. At the protein level, there is higher expression on the epidermis of the fish. When injecting a morpholino, a curly-down body axis with defected tails is formed, and the caudal vein of the fish seems to be affected.

This is the first report characterizing *cdkn2b* expression in Zebrafish embryos and in the correct formation of the tail and vessel mophology of the fish.

Key words: zebrafish, embryos, *cdkn2b*, development, aneurysms.

Table of Contents

Acknowledgements ii

Resumo v

Abstract viii

Chapter 1: Introduction 1

Chapter 2: Objectives 3

Chapter 3: State of Art 4

3.1 Cell cycle and INK4 family 4

3.1.1 *CDKN2A/ARF/CDKN2B* locus 6

3.1.2 Role of *CDKN2A*/*ARF*/*CDKN2B* locus in disease 7

3.2 Zebrafish animal model 9

3.2.1 Vascular Anatomy of early development of Zebrafish 11

3.2.2 Epidermis of Zebrafish 13

3.2.3 Zebrafish as a model for study human disease 14

Chapter 4: Materials and Methods 18

4.1 Zebrafish husbandry 18

4.2 Whole-Mount *In situ* hybridization 18

4.2.1 RNA Probe Synthesis 18

4.2.2 Whole-mount *in situ* hybridization in Embryos 19

4.2.3 Imaging 19

4.3 Immunohistochemistry 20

4.3.1 Whole-mount Imunohistochemistry in Embryos 20

4.3.2 Imaging 20

4.4 Morpholino Microinjection 21

4.4.1 Preparation of morpholino and microinjection 21

4.4.2. Rescue of phenotype by mRNA Injection 22

4.4.3 Imaging 23

4.5 Statistics 23

Chapter 5: Results 24

5.1 Expression of *cdkn2b* during zebrafish development 24

5.1.1 mRNA expression of *cdkn2b* 24

5.1.2 Protein expression of *cdkn2b* 25

5.2 Development of zebrafish embryos in absence of *cdkn2b* 29

5.2.1 Influence of *cdkn2b* in correct body axis and tail formation during zebrafish development 29
5.2.2 Vessel formation in the absence of *cdkn2b* during Zebrafish development 37
Chapter 6: Discussion 43
Chapter 7: Future Perspectives 47
Bibliography 48

Chapter 1: Introduction

Subarachnoid hemorrhage (SAH) is a life-threatening event that most frequently leads to severe disability and death. Its most frequent cause is the rupture of an intracranial aneurysm (IA), which is a dilation of a blood vessel caused by disease or weakening of the vessel wall. According to estimates, it affects approximately 2% of the general population and has devastating consequences to the quality of life of patients [1]. Therefore, IA diagnosis before rupture is of paramount importance. Despite recent advances in molecular techniques, mechanisms of IA initiation, progression, and rupture are still poorly understood.

Association between chromosome 9p21 and IA was shown by Helgadottir et al. [2] in different European populations and by Hashikata et al. [3] in the Japanese population. Importantly, 9p21 was also shown to be associated with other vascular phenotypes, such as coronary artery disease [4], ischaemic stroke [5], and aortic aneurysms [2], however the molecular mechanism underlying these associations has not yet been identified.

Despite the incredible amount of work done in the last years to understand IA genetic etiology, it has been particularly difficult to reveal the molecular basis of human aneurysms.

CDKN2B (cyclin-dependent kinase inhibitor 2B), also known as *INK4b* or $p15^{INK4b}$, is one of the members of INK4 family (CDK inhibitors)[6], and it is one of the genes present in the locus in 9p21 that were associated with IA [2]. This gene is also known for its role in cell aging, proliferation, and function as a tumor suppressor. However, the possible role in blood vessels and importance for the mechanisms underlying IAs is still not known [7].

To overcome the complexity of human genetic etiology, insights from animal models can also contribute to reveal the pathogenic mechanisms underlying IAs. Many researchers who are interested in an embryologically and genetically tractable disease model have now turned to zebrafish. Since there is an ortholog of *CDKN2B* in zebrafish (*cdkn2b*) we choose to use this model in our studies.

Zebrafish have a unique combination of genetic and experimental embryologic advantages that make them ideal models. Besides being a vertebrate, and thus closer to human than invertebrate models, has high fecundity (a few hundred eggs per spawning) and the embryos are transparent and develop externally. Unlike the embryos of many other vertebrates, zebrafish embryos are accessible to observation and manipulation at all stages of their development. Their generation time is short (2-3 months). In addition, adult zebrafish can be easily visualized and experimentally manipulated. Another advantage is that the zebrafish genome is being sequenced and genomic data is readily accessible. All these features,

previously found mainly in invertebrate models, facilitate genetic and high-throughput functional studies [8,9].

Compared to other vertebrate models, screens for zebrafish mutants are less costly and easier to perform. Large-scale mutagenesis screens have been performed in zebrafish allowing a better understanding of various human conditions. Zebrafish have also proven to be a particularly relevant vertebrate model for the study of human diseases, like DiGeorge syndrome due to zebrafish *van gogh* mutant [10].

Besides all the advantages of the zebrafish model for studying vertebrates' development as gene function, zebrafish has also become a good model system to study vascular biology. On one hand, forward genetic screens in zebrafish identified a number of fascinating vascular phenotypes. On the other hand, the transgenic lines of fish carrying an endothelial cell promoter-driven reporter like GFP (e.g. *fli1a:EGFP* zebrafish) [11], has allowed for the mapping of the zebrafish vasculature in detail with vascular processes amenable to real time visualization. These technologies, and evolving tools in reverse genetics, have led to the identification of numerous genes linked to vascular pathology, some of which phenocopy diseases seen in humans.

In these context, with zebrafish, we can test how a large number of IA susceptibility candidate genes influence IA pathogenesis.

Since at the beginning of the present study there were no information about *cdkn2b* (the ortholog of the human *CDKN2B*) during zebrafish embryo development, we started our project by characterizing this gene during zebrafish development using diverse techniques like whole-mount *in situ* hybridization and Immunohistochemistry. Functional studies were also performed using injection of antisense morpholino oligonucleotides (Mos).

To the best of our knowledge this is the first work characterizing *cdkn2b* during zebrafish embryo development and studying its possible involvement with vessel formation.

Chapter 2: **Objectives**

The main goal of the present dissertation was to characterize the *cdkn2b* gene during zebrafish development and to study its possible involvement/role during vascular development.

In order to accomplish that, we specifically proposed to:

1. Characterize for the first time the expression pattern of mRNA and protein levels of *cdkn2b* in zebrafish embryos;
2. Perform knockdown experiments using morpholinos against *cdkn2b*;
3. Analyze in detail the effect of *cdkn2b* knockdown on zebrafish blood vessels morphology;

Chapter 3: State of Art

3.1 Cell cycle and INK4 family

Cells can differentiate, commit suicide, or undergo cell division in response to internal and external demands. If cells proliferate, they go through the cell cycle, entering the G1, S, G2 and M phases. Coordination of these complex processes needs a tight regulation that involves several proteins present in the cytoplasm of the cells, like cyclins and cyclin-dependent kinases [7,12].

When exposed to appropriate stimuli, cells proliferate and enter in G1 phase, increasing in size and becoming ready for DNA synthesis (S phase). Between the end of S phase and the beginning of mitosis, cells enter in G2 phase, which allows cells to repair replication errors and prepare for mitosis (M phase). After completion of mitosis, a cell can exit the cell cycle and enter a state of quiescence, the G0 phase [7,12,13].

Progression from one phase to the next is regulated by cyclin-dependent kinases (CDKs) which make complexes with the appropriate cyclins, and regulate the cell cycle by their serine/threonine kinase activities. During the cell cycle, at specific time points, CDKs have to be activated or inactivated in an intricate manner, so that cell division can occur[7,12,14].

There are three checkpoints in the cell cycle. The late point in the G1 phase, called restriction point, involves many signals converging, namely the activity of CDKs, cyclin-dependent kinase inhibitors (CDKIs), and external signals like growth factors. According to the integration of these signals, the cell decides to stop proliferating or to progress towards mitosis [7,12,14].

Cyclin-dependent kinase inhibitors (CDKIs) mediate inhibition of the cyclin-CDK complexes and are divided in two different families, the CIP/KIP family and the INK4 family. The CIP/KIP family is formed by three members, $p21^{CIP1/WAF1}$, $p27^{KIP1}$ and $p57^{KIP2}$ and is able to inhibit the activity of all CDKs. The INK4 family has four members, *CDKN2A* (also known as $p16^{INK4a}$) [15], *CDKN2B* ($p15^{INK4b}$)[16], *CDKN2C* ($p18^{INK4C}$)[17], and *CDKN2D* ($p19^{INK4d}$) [18] which exclusively bind to and inhibit the CDK4 and CDK6. INK4 are proteins with about 15 to 19kDa and are highly conserved among species. In the same species, members of INK4 family share about 40% homology with one another [7,12].

In quiescent cells, CDK4 (or CDK6) form complexes with HSP90/CDC37 (a chaperon complex) and $p27^{KIP1}$ (or $p21^{CIP1/WAF1}$) form complexes with cyclins 2 (E-CDK2 or A-CDK2) and CDK2 which are inactivated. Progression through G1 phase of the cell cycle is induced by

mitogen binding to receptors that activate multiple signaling pathways, converging on the transcription of immediate early genes (D-type cyclins) and cyclin assembly to CDK4/6 kinases [6, 15, 19].

In the G1 phase of the cell cycle, $p27^{KIP1}$ is released from cyclin E-CDK2 complexes and binds to new complexes with cyclin D and CDK4, releasing inhibition of cyclin E-CDK2 complexes and activating cyclin D-CDK4 complexes, both of which then phosphorylate the retinoblastoma protein (pRB). P27 itself is also phosphorylated by cyclin E-CDK2 complex, leading to its degradation. Once phosphorylated, pRB releases tethered E2F transcription factors, leading the cells to enter in the phase S of the cell cycle [6, 15, 19, 20].

The INK4 family is responsible for the arrest of the cells in G1 phase in a pRB-dependent manner. CDK4 is redistributed from cyclin D-CDK4 complexes to form INK4-CDK4 complexes. Cyclin-D is then degraded by the ubiquitin/proteasome pathway. With the decrease of cyclin-D, $p27^{KIP1}$ keeps cyclin E-CDK2 sequestered, preventing pRB phosphorylation and thus promoting the arrest of the cell in G1(Fig. 3.1) [6, 15, 19, 20].

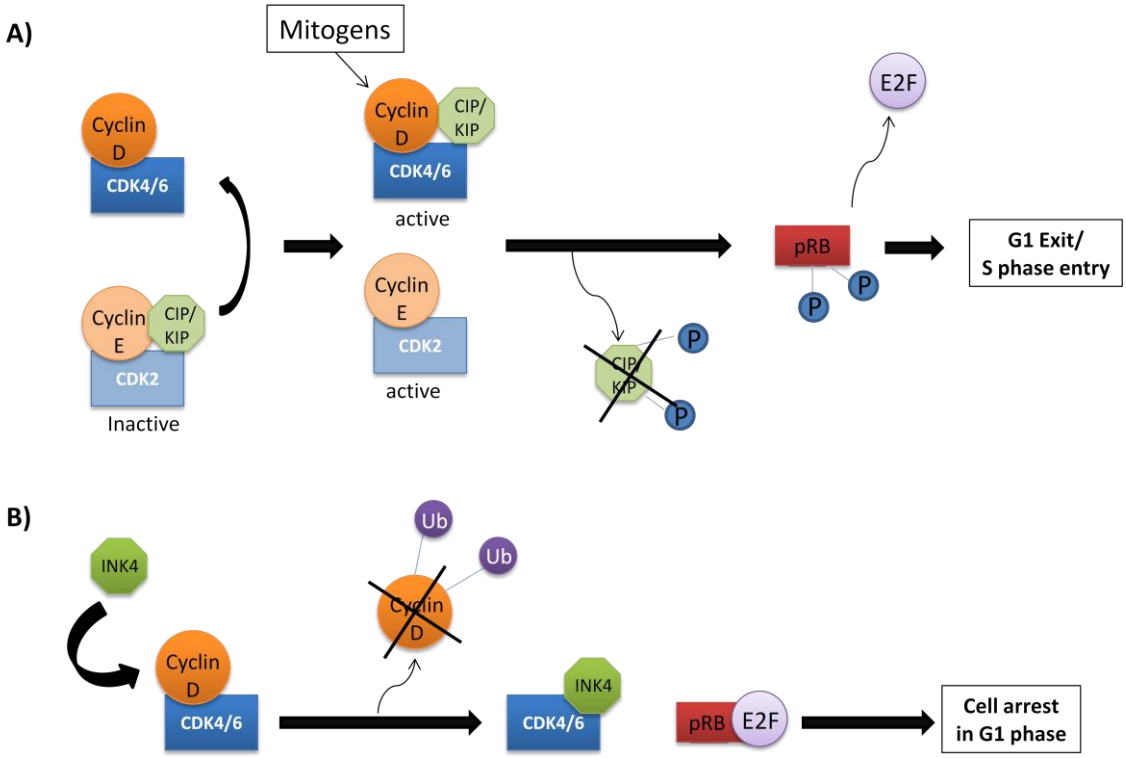

Figure 3.1 - Schematic representation of G1 progression and arrest of cell progression duo to INK4 family. A) Mitogens regulate the expression of D-type cyclins and their assembly to CDK4/6. In early G1 phase, the cyclin E-CDK2 (or cyclin A-CDK2) complexes are inhibited by bound to a member of CIP/KIP family ($p27^{KIP1}$ or $p21^{CIP1)}$. As cyclin D expression rises in response to mitogens, it forms complexes with CDK4 or CDK6 and $p27^{KIP1}$ or $p21^{CIP1}$. This unleashes cyclin E and A-CDK2 catalytic activity, allowing further pRB phosphorylation and releasing of transcriptor factor E2F; G1 exit and S phase entry. B) INK4 proteins specifically bind to and inhibit the cyclin D-dependent kinases, CDK4 and CDK6, leading to cyclin-D degradation and cell arrest in G1 phase.

The role shared by INK4 proteins in sequestering both CDK4 and CDK6 might explain why the deletion of a single INK4 member does not always lead to phenotypic effects [7,12].

As mentioned before, *CDKN2B* is one of the four known members of the INK4 family. It is mostly found in the cytoplasm of the cell, and in agreement with other proteins of the INK4 family it is able to arrest the cell in G1 phase [7,12].

TGF-β specifically induces an increase in a subset of CDKIs expression, including *CDKN2B*, $p21^{CIP1}$, and $p27^{KIP1}$. TGF-β causes the up-regulation of *CDKN2B* mRNA, and increased binding of the protein to CDK4 and CDK6 in epithelial cells, thus leading to cell arrest [20,16,21].

3.1.1 *CDKN2A/ARF/CDKN2B* locus

CDKN2B encompasses 6.41 Kb of DNA, has 2 coding exons and can be found on the chromossome 9p21 (in humans) [22]. In the mouse, the ortholog of this gene can be found in the chromosome 4 [23]. *CDKN2B* is located in a locus conserved in mammals and commonly referred as *CDKN2A/ARF/CDKN2B* locus (Fig. 3.2). This locus has been largely implicated with susceptibility to several diseases and encodes for three products, *CDKN2A, ARF* and *CDKN2B* [24,25,26]. *CDKN2A* and *CDKN2B* genes codify for the CDKN2A and CDKN2B proteins, respectively. CDKN2A and CDKN2B degree of relatedness suggests that they arose as the result of a tandem duplication. The third product, ARF, expressed from a distinct promoter and an alternative reading frame of *CDKN2A*, inhibits the activity of the oncoprotein MDM2 and activates p53 [25,26,27].

Besides the genes referred before, initiated from the CDKN2A-ARF-CDKN2B gene cluster, we can also find *ANRiL* (antisense non-coding RNA in the INK4 locus). *ANRiL* is a transcript that may be involved in the repression of *CDKN2A*, *ARF* and/or *CDKN2B*. Exon 1 of *ANRiL* locates between the promoter of *ARF* and *CDKN2B*, and is transcribed in the direction opposite from *CDKN2B* [25, 28,29,30].

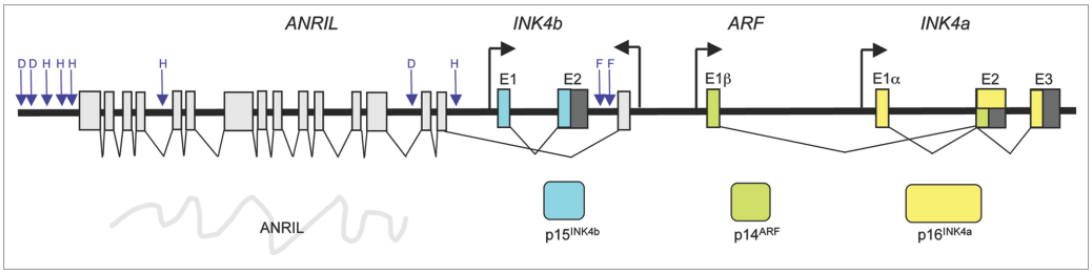

Figure 3.2 - Organization of the human *CDKN2A/ARF/CDKN2B* locus (previously known as INK4b/ARF/INK4a locus) and disease-associated SNPs. The coding exons are shown in colors and non-coding exons are shown in light gray for ANRiL and dark gray for the other genes of the locus. The approximate position of single nucleotide polymorphisms (SNPs) associated with disease states is indicated by blue arrows. SNPs associated with type 2 diabetes mellitus (D), vascular heart disease (H) and frailty (F) are indicated. Map is not drawn to scale and positions are approximate (adapted from N. Popov, 2010 [25]).

3.1.2 Role of *CDKN2A/ARF/CDKN2B* locus in disease

Besides the importance of *CDKN2A, CDKN2B and ARF* in cell proliferation, there is evidence for an extended role of the *CDKN2A/ARF/CDKN2B* locus as tumor suppressors and in conferring susceptibility to some diseases [25].

_i_) Role of *CDKN2A/ARF/CDKN2B* as a tumor suppressor

The capacity of *CDKN2B*, *CDKN2A* and *ARF* to block cell proliferation gives them appropriate biochemical properties as tumor suppressors [25].

The *CDKN2A/ARF/CDKN2B* locus is deleted in a wide variety of tumors including melanoma, pancreatic adenocarcinoma, glioblastoma, leukemias and bladder carcinoma. In many human cancers there is a homozygous deletion of the *CDKN2A/ARF/CDKN2B* locus that eliminate the expression of all the three proteins codified by the locus. Many studies have been performed in order to discover which of the three proteins represents the main tumor suppressor activity located at the locus. In many human cancers specific somatic loss of *CDKN2A* without affecting *CDKN2B* or *ARF* are known to be present, however, specific genetic lesions of *CDKN2B* without affecting *CDKN2A* or *ARF*, are still not very well described [6, 25].

Mouse models have also confirmed that deficiency for either of the proteins encoded by the *CDKN2A/ARF/CDKN2B* locus, alone or in combination, results in tumor-prone animals. Overexpression of the *CDKN2A/ARF/CDKN2B* locus in mice also supports its role in tumor suppression [6,31].

Moreover, it was also demonstrated that hypermethylation of *CDKN2B* gene caused specific epigenetic silencing in rare glial tumors and certain hematologic neoplasma including leukemia and myelodysplasia. In myelodysplasia, *CDKN2B* hypermethylation has been

reported in the absence of *CDKN2A* hypermethylation and in some of these cases the expression of *CDKN2B* can be reactivated in response to treatment with inhibitors of DNA methyltransferase. Furthermore, because of their overlapping biochemical function, co-deletion of *CDKN2B* with *CDKN2A* may be more oncogenic in certain tissues than loss of either alone [6] .

In conclusion, *CDKN2A/ARF/CDKN2B* locus encodes three tumor suppressors which together constitute one of the main anti-oncogenic defenses of mammalian organisms.

***ii*) *CDKN2A/ARF/CDKN2B* locus – multiple genome-wide association studies (GWAS)**

In the last years, numerous studies have implicated the *CDKN2A/ARF/CDKN2B* locus with increased susceptibility to several diseases, like coronary artery disease (CAD) [4,32,33,], Intracranial aneurysms [3,34], myocardial infarction [35,36], type 2 diabetes [30] or Alzheimer disease [37].

Most of these evidences came from GWA studies in which SNPs located in a region spanning 120kb around the *CDKN2A/ARF/CDKN2B* locus presented significant association with a disease. Interestingly, on those studies, different SNPs on the same region have been associated with increased disease risk. This suggests that the increased susceptibilities observed are the responsibility of several polymorphisms [38].

Although until now most of these SNPs were not directly linked to a particular gene, they were located inside the locus close to *CDKN2A* and *CDKN2B*, suggesting a possible regulatory role of these genes in the process.

One of the best studied examples of association of a disease with *CDKN2A/ARF/CDKN2B* locus has been with coronary artery disease (CAD). A 58kb region on chromosome 9p21 has consistently shown strong association with CAD in populations of North American and Northern Europe [39], as well as were replicated in South Korean, Japanese [40], American Hispanic [41], Chinese [32] and Italian populations [36]. Curiously, the same region that showed strong association with CAD was also associated with the presence of Abdominal Aortic Aneurysm [2], which suggest that the effect of this locus on risk of cardiovascular disease extends beyond the coronary circulation.

Also in this studies, a robust association between 9p21 and *ANRiL* was demonstrated. There is an hypothesis referring that lower expression of *ANRiL* modulate cell growth, possibly via *CDKN2A* and *CDKN2B*. However, there will be needed further investigation to know what the association between chromosome 9p21 and CAD [28, 29,30].

Like was referred before, Intracranial aneurysms are balloon-like dilations of the intracranial arterial wall and their hemorrhage commonly results in severe neurologic impairment and death [42,43]. Also in this case, a SNP near *CDKN2B* was associated with IAs in two European and one Japanese populations [2,3]. However, the mechanism behind the process is still unknown. Using a murine model it was discovered that alterations in TGF-β signaling are associated with aortic dilatation during the early stages of thoracic aortic aneurysm development, by inducing matrix degradation, but no data exists on intracranial aneurysms [44]. As was refer before, TGF-β can induce an increase in *CDKN2B*, however no direct relationship among TGF-β, *CDKN2B* and intracranial aneurysms is known.

Although zebrafish have many advantages has a model and an ortholog of *CDKN2B (cdkn2b)* exists, this model has never been used to study the importance of *cdkn2b* in IAs. *cdkn2b*, in zebrafish, is present in the chromosome 1, it is formed by 2 exons and 1 intron and codifies for a protein with a length of 125 amino acids (Zfin, http://zfin.org).

3.2 Zebrafish animal model

Zebrafish (*Danio rerio)* are small tropical fish native from Southeast Asia that belongs to the minnow family (Cyprinidae) of order Cypriniformes [45].

Due to the combination of its genetic and experimental embryologic advantages, the zebrafish is a prime model for genetic and vertebrate developmental studies.

Zebrafish breed prodigiously with short time generations and are easy to maintain. Once fertilized, the zebrafish embryo (Fig. 3.3) rapidly develops, within a protective chorion, from a single cell situated on the top of a large ball of yolk, to the thousand-cell blastoderm only four hours later. By the end of 24hpf (hours post fertilization), organogenesis has begun; it starts acquiring pigmentation, the major organs have visibly formed, and the embryo has begun to adopt a more familiar shape. At about 48 hours post fertilization, the embryo hatches, breaking free of the chorion, and begins to swim and eat. At 72hpf the mouth is open, the blade of the pectoral fin continues to expand to the posterior over most of the yolk ball, that continues to diminish. After 72hpf, the fish is considered a larva and continues to increase its size. At 30-44dpf it is considered a juvenile and in 2-3 months post-fertilization it is an adult [46].

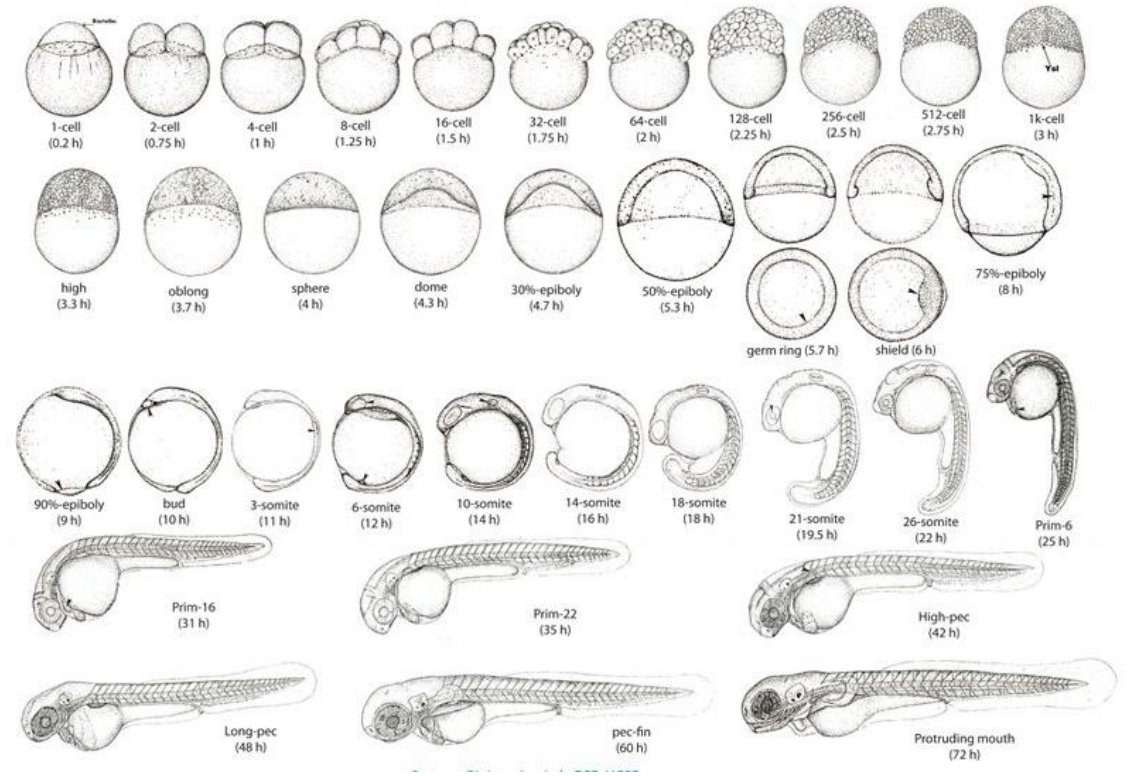

Figure 3.3 - Stages of development of zebrafish embryo. The animal pole is the top for the early stages, and anterior is on the top later, except for the two animal polar (AP) views shown below their side view counterparts for germ-ring and shield gastrulas. Face views are shown during cleavage and blastula stages. After shield stage, the views are of the embryo's left side, but before the shield arises one cannot reliably ascertain which side is which. Pigmentation is omitted. Arrowheads indicate the early appearance of some key diagnostic features a the following stages: 1 k-cell: YSL nuclei. Dome: the doming yolk syncytium. Germ ring: germ ring. Shield: embryonic shield. 75Oh-epiboly: Brachet's cleft. 90%-epiboly: blastoderm margin closing over the yolk plug. Bud: polster. 3-somite: third somite. 6-somite: eye primordium (upper arrow), Kupffer's vesicle (lower). 10-somite: otic placode. 21-somite: lens primordium. Prim-6: primordium of the posterior lateral line (on the dorsal side), hatching gland (on the yolk ball). Prim-16: heart. High-pec: pectoral fin bud. (from http://www.ece.ucsb.edu/~sandeepkbhat/downloads.html).

The fact that zebrafish is transparent and has externally developing embryos allow easy transient genetic manipulation and imaging analysis. All the major organs of the embryo can in this way be easily observed, including the major divisions of the brain, the neural tube, floorplate, notochord, somites, heart, jaw, gills, liver and gut [8].

Especially advantageous for the study of zebrafish development, is also the use of transgenic lines that express a fluorescent protein, such as green fluorescent protein (GFP). This protein is usually under the control of an organ-specific promoter and is very useful to monitor the development of a given organ, like for instance is the case of the study of vascular development [11].

3.2.1 Vascular Anatomy of early development of Zebrafish

Anatomically, vascular development in zebrafish proceeds in a mode analogous to what is observed in other vertebrates [47].

In the zebrafish embryo, circulation begins at approximately 24hpf, through a simple single circulatory loop. Blood exits the heart in direction to the mandibular aortic arches in the head, returning by the lateral dorsal aortas to the trunk, merging in a single medial dorsal aorta (DA) and finishing in the caudal artery (CA) at the tail of the fish. Then, returns by the caudal vein (cv) continuing to the trunk by the posterior cardinal vein (PCV) and entering again in the heart of the fish. Shortly after the commencement of this initial circulatory loop, at approximately 24hpf-36hpf, a second cranial circulatory loop is formed and intersegmental vessels (Se) start to develop (Fig. 3.4A) [48,49] .

By 48hpf, the major arterial and venous pathways of the head are apparent and most trunk and tail Intersegmental vessels have already lumenized and possess an active circulation (Fig. 3.4B). At the head, the main arterial route for the brain, consisting in the Primitive internal carotid artery, the Caudal division of the internal carotid artery (CaDI), and Basilar artery (BA) becomes robust and new branches appear from these vessels. Also at this stage, the dorsal longitudinal anastomotic vessels (DLAVs) are still two paired vessels disposed cranially, but caudally it diverges through many anastomotic vessels that are present between the right and left DLAVs. The supraintestinal artery (SIA) and the subintestinal veins (SIV), which will eventually provide blood supply to the digestive system, begin to appear and in the aortic arch system, the third and forth aortic arches appear.

Despite massive elaboration of smaller caliber vessels in the head through the next days, the overall “wiring” pattern of major head vessels is largely unaltered after 48–60 hpf. Also at this moment (60 hpf), the fifth and the sixth aortic arches start to develop and the complete set of aortic arches is present. Meanwhile, increased dorsal-ventral separation begins to appear between the axial vessels (DA and PCV), a process that will continue at least through 4.5 dpf and the Caudal vein (cv) plexus continues to slowly condense down into a single more ventral channel. Also at this stage, a caudal circulatory loop is formed between the CA and the base of the caudal fin [48,49].

Next stages are mainly characterized by the appearance of multiple venous connections linking to the organs in development, like for instance, to the liver or the gills.

At 72hpf, the vascular plexus of the mid- and hindgut walls starts to appear (Fig. 3.4C). Additionally, the aortic arches start to divide into afferent and efferent branchial arteries continuing the process for the next several days. Also at this stage, the hypobranchial artery

(HA) appears, the one responsible for providing blood supply to the ventral branchial region and the heart. At the caudal trunk and tail, the DLAVs are just beginning to form a simpler single plexiform vessel and, although at this point, the basic pattern of trunk and tail intersegmental vessels (Se) is established, two additional types of trunk vessels extend horizontally (anterior-posterior) from the Se: the primordial vertebral artery (VTA) and the parachordal vessel (PAV). The first one sprouts more dorsally and the other one, more ventrally. Nevertheless, they only begin to progress in order to span the somites at 4-5 dpf.

Although many additional cerebral capillaries continue to form in the head through next stages, and exiting vessels may be significantly remodeled, the basic wiring plan of major vessels already established is still maintained at later stages [48,49].

The use of transgenic lines that express GFP in the vessels, *fli1a:EGFP* [50] allows *in vivo* imaging analysis and provides easier means to find alterations in mutants, such as in large scale mutagenesis screens.

fli1a:EGFP transgenic fish have been where very important in the characterization of zebrafish vascular development. As well as in the study of some diseases. For example, the *fli1a:EGFP* transgenic allowed to study the Von Recklinghausen neurofibromatosis disease by studying zebrafish *nf1a* and *nf1b*, orthologues of *NF1.* Von Recklinghausen neurofibromatosis is caused by mutations in the *NF1* gene, which encodes neurofibromin [51].

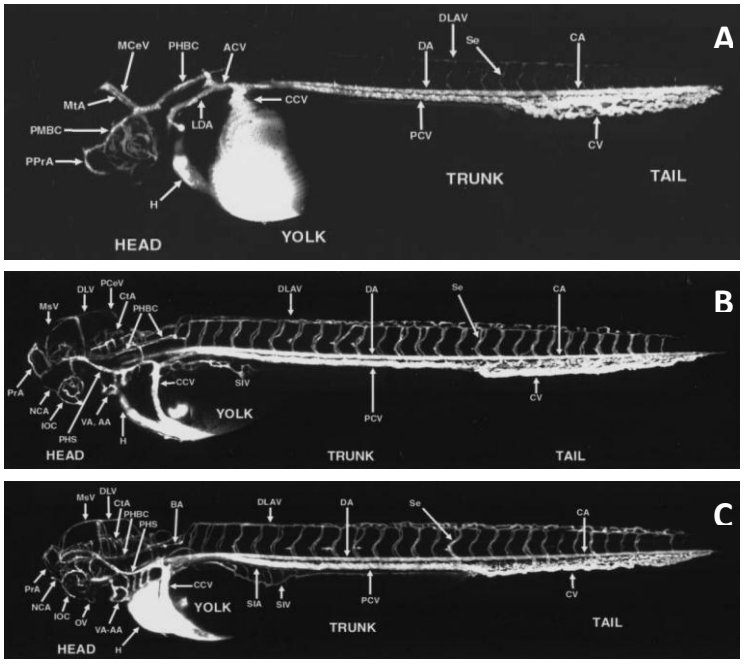

Figure 3.4 - Circulation in the developing zebrafish at approximately 24-36hpf (A), 48-60hpf (B) and 72-84hpf (C). Angiogram of a developing zebrafish, compiled from four separate reconstructions pasted together. Lateral view, labeled. (Adapted from Isogai et al, 2001 [52]).

3.2.2 Epidermis of Zebrafish

The epidermis is a barrier between the internal organs of an organism and its environment and the biggest organ of vertebrates. It is a first-line defense system against pathogens [53].

In adults, epidermis is formed by three layers, the surface, intermediate and basal layers. The surface layer is a single cell layer that develops microridges at the outer surface. Microridges are raised, actin-rich structures that serve to maintain a mucous layer on the surface of the fish. Contrary to terrestrial vertebrates whose outer layer of epidermis is formed of keratinized dead cells, in zebrafish this layer is formed by living keratinocytes covered with mucus. These cells are not periodically renewed, but replaced individually by cells from the intermediate layer on cell death [53,54,55].

The intermediate layer is composed of various types of cells with different functions: unicellular, sensory cells, ionocytes, and the most dominant, undifferentiated cells. Most cells in this layer are undifferentiated, providing a source of keratinocytes to replace dead or wounded cells. At last, the basal part of the epidermis consists in a single cell layer attached to the basement membrane via hemidesmosomes. This layer is responsible for linking epidermis to dermis [53,54].

Cells of epidermis are differentiated very early during embryonic development. The epidermis of the zebrafish embryo is constituted by two cell layers which are formed at different developmental stages and become the simple epithelium of the embryo. The surface layer of the embryo, called enveloping layer (EVL), is formed by keratinocytes and is similar to the periderm of mammalian embryos, both morphological and functionally (Fig. 3.5). In mice and humans, keratinocytes are known to express *CDKN2B* in response to TGF-β expression.

The inner layer called epidermal basal layer (EBL) is different from the basal layer of adult epidermis because contains both differentiated and undifferentiated cells [53,54,55].

At approximatly 10hpf, EVL is replaced by periderm. Later in development, at about 24hpf, the superficial stratum of the epidermis replaces periderm. Superficial stratum already has the same properties of the outer layer of epidermis in the adult fish [53,54,55].

By 72hpf the epidermis has begun the differentiation process and comprises two layers: a basal epidermal layer contacting a basement membrane, and a surface layer decorated with microridges. The epidermis of the fish continues to develop until the three layers present in the epidermis of an adult fish are formed [53,54,55].

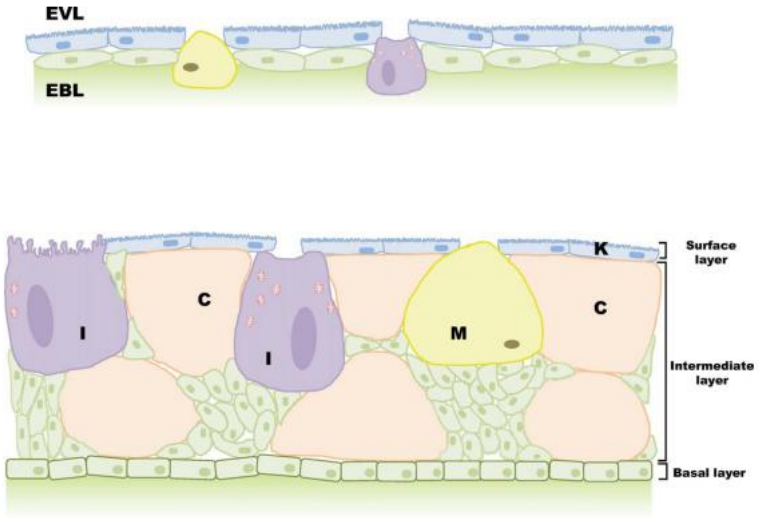

Figure 3.5- Structure of embryonic (upper panel) and adult (lower panel) epidermis of zebrafish. The embryonic epidermis is formed by outer EVL and inner EBL, and adult epidermis is formed by surface layer, intermediate layer and basal layer. Surface layer and basal layer are single cell layers that are composed of keratinocytes (K) and undifferentiated cells, respectively. Intermediate layer is composed of mucous cells (M), club cells (C), ionocytes (I), and undifferentiated cells (adapted from Wei-Jen Chang et al, 2011 [56]).

3.2.3 Zebrafish as a model for study human disease

Although this model has been under investigation for more than half a century it has emerged recently as a powerful vertebrate model to study human diseases. Molecular events that orchestrate a variety of morphogenesis and organ formation in humans are known to be conserved in zebrafish [8,9].

Zebrafish has been used as a model for human diseases specially in carcinogenesis, infection and inflammation, in the discover of genes related with genetic diseases and in the area of new drug discovery [8,9].

In carcinogenesis, the model can be used as a tool to understand the functional importance of genes present in human cancer. For instance, the Zebrafish model was used to study *SETDB1*, an amplified and over expressed gene in human melanoma [57].

The Zebrafish model can be used in the context of infection and inflammation to investigate the genes that are involved in host defense mechanisms. It can also be used to study the importance of cellular components of the inflammatory response. For instance, transgenic zebrafish with GFP-marked macrophages [58], neutrophils [59], and endothelia [11] have been used to investigate sterile acute inflammation caused by wounding [8,9].

In the area of new drug discovery, the zebrafish model is important because it is the premier whole-animal vertebrate used for the search of compounds with desired therapeutic bioactivity. Through the use of transgenic or mutant zebrafish that manifest a particular

disease phenotype, it is possible to identify compounds capable of suppressing diseases. For instance, the *gridlock* mutant phenotype is very similar to a common human congenital disorder termed *coarctation of the aorta*, and this mutant was used in order to screen small-molecules capable of suppressing this phenotype [8,9,60].

One of the main contributions to the study of diseases and its mechanisms of action has been the advantage of performing gain or loss-of function experiments in zebrafish [8,9].

A recent addition to the zebrafish genomic toolbox was the development of morpholinos (Mos). This experimental approach is based on microinjection of Mos into one-cell stage embryos and is commonly used to temporarily silence zebrafish genes during the first few days of embryonic development [61,62].

i) The use of Morpholinos in zebrafish to knockdown a protein

Mos are chemically modified oligonucleotides that can specifically bind to their target mRNAs with more stability and resistance to endogenous degradations. They normally have 25 nucleotides with morpholine rings in their backbones instead of the deoxyribose rings in DNA or ribose rings in RNA. Mos carry A, C, G or T bases positioned according to Watson-Crick base pairing and, instead of the anionic phosphodiester linkage found in DNA or RNA, contain uncharged phosphorodiamidate intersubunit linkages [61,63,64].

Their hybridization to mRNA can block translation when they are targeted to sequences near the translation initiation codon, the so called translation-blocking morpholinos. Or, they can block splicing when targeted to exon-intron boundaries and are called splicing-blocking morpholinos. This method has proven to be simple, rapid, specific and effective [65,66,67,68].

The effectiveness of Mos can be evaluated using Western blotting or immunohistochemistry when using translation-blocking morpholinos with specific antibodies against the protein of interest. Alternatively, when using splicing-blocking morpholinos, we can use Reverse Transcription-PCR with primers spanning the altered splicing region.

There are some limitations to the use of Mos. On one hand, the effectiveness of Mo can only last 3-5 dpf. Due to the quick cell proliferation during embryogenesis, the injected Mo is too diffused to effectively bind to their cellular targets after 5 dpf. On the other hand, Mos can induce some phenotypes resulting from their toxicity and off-target effects [61,63,64,65].

In order to use this technique correctly many controls are needed. Usually, two different Mos are used to define the shared phenotypes, which may be specific effects of the Mo. Custom control Mos includes mismatch Mos, which have nearly the same sequence as

the antisense Mo sequence but incorporates five mismatches along the length of the oligo. Alternatively, Standard control Mo are routinely used. Standard control Mo targets a region on human pre-mRNA, and has no target and no significant biological activity in zebrafish. These controls can be used to isolate Mo off-target effects [65,66,67,68].

Another control usually used when injecting Mos is the co-injection with p53 Mo. Neural death caused by Mo-induced off-target effects is frequent. For instance, injecting a splice-site wnt5 MO (against *wnt5/pipetail*) not only induces tail and body-axis shortening and somite compression, characteristic of the *wnt5/ppt* mutant, but it also induces neural death, which is uncommon in the mutant resulting from activation of p53 (Fig. 3.6). This neural death was proven to be the result of off-target effects of the wnt5 MO and was classified as middle, intermediate or severe [68,69].

p53 Mo knockdown by itself does not induce any significant defects, as p53 is not required for normal development in the fish. p53 Mo can be used as a tool to alleviate off-target neural death. Also, p53 Mo does not affect the efficacy of gene-specific Mos, because it does not interfere with the penetrance of gene-specific phenotypes. p53 Mo can be co-injected with the Mo of interest and it is usually injected 1.5-fold (w/w) to the other Mo used [68,69].

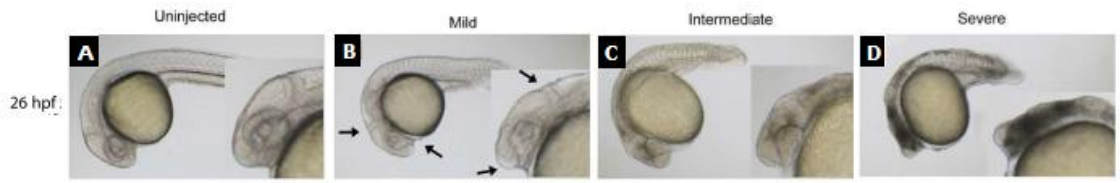

Figure 3.6 - Representative cell death phenotypes detected at 26 hpf caused by Mo-induced off-target effects with different levels of severity. Zebrafish embryos not injected (A) and injected with Wnt5 Mo1 (B,C and D). Lateral views with inserts showing a higher magnification of the head region (Adapted from Robu et al, 2007 [69]).

Rescue of Mo induced phenotypes by injection of mRNA encoding the protein of interest can also help to establish whether the phenotypes are specific of the Mo. Ideally, mRNA injected must have 5 mismatch at the region where Mo binds, without altering the reading frame. This prevents the Mo to bind to the mRNA synthesized. However, mRNA without mismatches can be used, although have some disadvantages. The microinjection of the mRNA without mismatches may require a more rigorous titulation to find the right amount of mRNA needed.

Occasionally, when injecting mRNA at one cell stage embryos we are including mRNA of a gene in tissues where it is not express, or are increasing the expression of this gene. This

can cause some side effects. Sometimes, due to side effects of the microinjection of mRNA of the gene of interest it is not possible to do a successful rescue of a phenotype [68,69].

Chapter 4: **Materials and Methods**

4.1 Zebrafish husbandry

The embryos were obtained from crosses between adult zebrafish, *Danio rerio*. The *wild-type (wt) AB* embryos resulted from crossing the *wild-type AB* strain. The *fli1a:EGFP* zebrafish, a transgenic that has the blood vessels marked with GFP, were the result from a cross of a *fli1a:EGFP* heterozygous male and a *wild-type AB* female. The crosses were made by putting single mating pairs together overnight in crossing boxes separated by a divisory. Partitions were removed in the morning and the eggs were collected and kept at 28ºC in embryo medium 1x (obtained from stock solution 50x - 2,43g $CaCl_2 2H_2O$, 0.63g KCl, 14.69g NaCl, 4.07g $MgSO_4 7H_2O$ with 1ml methylene blue per 10L of final solution) until reaching the desired developmental stages.

4.2 Whole-Mount *In situ* hybridization

Whole-Mount *In situ* hybridization is a powerful tool for visualizing gene expression patterns in specific cells and tissues. This technique allowed us to characterize expression of *cdkn2b* mRNA at different stages of development of *wild-type* AB zebrafish using specific digoxigenin-labeled RNA probes.

4.2.1 RNA Probe Synthesis

Plasmid containing *cdkn2b* gene (kindly provided by the Zebrafish Neurogenetics Department, Helmholtz Zentrum München, German Research Center for Environmental Health) was transformed into Top10 chemically competent cells. The transformed cells were planted along with 200µL of Ampicilline allowing to select the transformed cells. After selection, Mispeed Plasmid Purification Kit (QIAGEN, Venlo, Netherland) was used and followed the manufacturer's protocol. After purification and running the plasmid on a 0.8% agarose gel, it was quantified using Nanodrop spectrophotometer.

To digest the construct, 50µL of the plasmid was incubated in 30µL H_2O MiliQ (MQ), 10 µL of the appropriate restriction enzyme and 10 µL of appropriate buffer at 37ºC during overnight. To digest DNA for the sense probe, the restriction enzyme used was BamHI (Promega, Fitchburg, WI, USA), and for antisense probe it was used Hind III (Promega).

After digestion, the sample was run in a 0.8% agarose gel to confirm efficiency of digestion and then DNA was purified with the PCR Purification Kit (QIAGEN, Venlo, Netherland) following the manufacturer's protocol. After quantification using Nanodrop spectrophotometer, the construct was sequenced using Sanger method.

In order to transcribe the probe, the following reagents were mixed: 1µg of DNA template, 5µL of 5xBuffer Transcription (Promega), 1µL of DTT – (0,75mM), 2.5µL 10xDIG-NTPmix, 1µL of RNAsin, 1µL of DNA Polymerase (20U) (T3 polymerase (Promega) for sense probe and T7 (Promega) for antisense probe, respectively) and H_2O to a final volume of 25µL. The mix was incubated for 3hours at 37ºC, and then it was added 1µL of DNAse (Roche, Basel, Switzerland) and incubated at 37ºC for 15min. After transcription, the ProbeQuant G-50 Micro Columns kit (GE Healthcare, Uppsala, Sweden) was used to purified the probe and run the RNA in a 0.8% agarose gel.

4.2.2 Whole-mount *in situ* hybridization in Embryos

For the whole-mount *in situ* hybridization the protocol of Thisse and Thisse (2008) [70] was followed with some modifications. In order to prevent the formation of melanin pigments, for stages after 24hpf, the embryos were treated with 1-phenyl-2-thiourea (PTU, 0.03mg/mL) (Sigma, St. Louis, MO, USA). Embryos were manually dechorionated only after rehydration using forceps. Digestion with proteinase K was performed at 20 µg/ml in PBT solution [1X phosphate buffered saline (PBS) with 0.2% bovine serum albumin (BSA) and 0.1% Triton-X]. In order to reduce the background staining, 4mM of Levamisole hydrochloride (Sigma) was added to the staining buffer. After staining, the reaction was stopped by washing 3x5min with PBT and refixed in paraformaldehyde (PFA) 4% for 20min. Then, samples were washed in PBS 3x5min and incubated consecutively in: 25%glycerol in PBS, 50%glycerol in PBS and 75% glycerol in PBS. Finally, embryos were incubated in 100% glycerol overnight and then photographed.

As a negative control we used the sense probe and to test the expression of mRNA of *cdkn2b* we used antisense probe obtained as described before (section 3.2.1). As positive control we used a probe for *sox9b* kindly provided by another IMM Unit (UDEV). All the probes diluted were diluted (1:100) in HybMix (protocol of Thisse and Thisse (2008)).

4.2.3 Imaging

Embryos were photographed using a Leica Z6APO stereoscope equipped with a Leica DFC490 digital camera and pictures were produced using Adobe Photoshop and Illustrator.

4.3 Immunohistochemistry

Immunohistochemistry allows the localization of proteins in tissue by using labeled antibodies as specific reagents through antigen-antibody interactions that are visualized by a marker such as fluorescent proteins. This technique was important to characterize in which tissues cdkn2b is present.

4.3.1 Whole-mount Imunohistochemistry in Embryos

Embryos were fixed in the same manner as in the whole-mount *in situ* hybridization. Also to prevent the formation of melanin pigments, for stages after 24hpf, the embryos were treated with PTU (0.03mg/mL) (Sigma). Embryos were rehydrated by successive incubations (5minutes each) in: 75% methanol (MeOH) in PBS, 50%MeOH in PBS, 25%MeOH in PBS and 100% PBS. Then embryos were manually dechorionated using forceps and washed two times in PBS 1% triton (5minutes), one time in PBS (5minutes) and then permeabilized in acetone for 7minutes at -20ºC. The embryos were washed in PDBX solution (50%PBS pH7.3, 1%DMSO, 0.05%Triton X-100, 1mg/mL Bovine Serum Albumin in water MQ) and incubated in blocking solution (15 µL of goat serum per 1mL of PDBX) for 2 hours. Then after, embryos were incubated at 4˚C overnight with primary antibody diluted in blocking solution. Primary antibody used was rat anti-Ink4b (kindly provided from Zebrafish Neurogenetics Department, Helmholtz Zentrum München, German Research Center for Environmental Health) (1:100). The next day, the embryos were washed 4x30minutes in PBDX and incubated at 4˚C with secondary antibodies diluted in blocking solution. The secondary antibody used was Alexa Fluor 568 anti-rat (1:500). After this point, the tubes were protected from light using aluminum paper around the tubes. The embryos were washed 2x10 minutes in PBDX and 1x30 minutes in PBS. Then incubated in PBS with DAPI (10µL of DAPI per 10mL of PBS) and washed again 3x5minutes in PBS. Finally, the embryos were stored in mounting media (80% glycerol, 20% DABCO in PBS) at +4ºC in the dark.

As negative controls we performed the normal protocol using blocking solution instead of the secondary antibody in one control, and the primary antibody in another control.

4.3.2 Imaging

The embryos were mounted using a plastic ring with some silicon grease on the top and the bottom and pressed it onto a coverslip (24x24mm) forming a watertight seal. Embryos

were mount inside of the ring in 2% low melting agarose in embryo medium. After orientation of the embryo using forceps and once the agarose has set firm, enough PBS was pipette onto the surface of the agarose to form a convex meniscus over the top of the ring, and then took another slide and press down onto the top of the ring expelling the excess PBS.

Imaging was performed using a confocal point-scanning microscope (LSM710; Carl Zeiss), using a 20x dry, 40x oil and 63x oil lens. The pictures were analyzed using Fiji (ImageJ NIH) and Adobe Photoshop and Illustrator.

4.4 Morpholino Microinjection

Morpholinos oligonucleotides (Mos) are antisense oligos that bind to mRNA blocking translation. Microinjection of morpholinos in zebrafish embryos at one-cell stage is commonly used to alter gene expression. In the present study, this technique was used to discover if knockdown of *cdkn2b* causes a specific phenotype. Particularly, we are also interested to see if the knockdown of *cdkn2b* causes alteration in the formation of the vessels of the fish, therefore *wild-type* AB and transgenic *fli1a:EGFP* zebrafish were used.

4.4.1 Preparation of morpholino and microinjection

Mos used in this study were purchased from Gene Tools (Philomath, Oregon, USA) and are listed in detail in Table 4.1. A stock of 1mM was prepared diluting in H_2O MQ and after that, Mos were diluted to working concentrations. Prior to microinjection, morpholinos were pre-heated to 65^{o}C for ten minutes and then briefly vortex in order to assure that the oligos were completely dissolved.

For the microinjection, eggs from the fish were collected as described before (section 4.1.) and calibration of a fine glass needle was prepared to inject 1.4nL of each Mo per embryo. After injections, the embryos were stored in embryo medium at 28ºC until the desired time.

To discover what was the right concentration of morpholino to use in our studies, primary we injected embryos with different amounts of *cdkn2b* Mo (1.2ng, 1.8ng, 2.4ng, 3.6ng of *cdkn2b* Mo) and *cdkn2b* Mo2 (3.6ng, 6ng, 12ng of *cdkn2b* Mo2).

Besides the interest morpholinos (*cdkn2b* Mo and *cdkn2b* Mo2), several controls were also injected. We have co-injection *cdkn2b* Mo and *cdkn2b* Mo2 to test the specificity of the phenotype. For this co-injection we also had to test what was the right amount of morpholino

(we co-injected 1.2ng+6ng, 1.7ng+8.4ng). As a control for the injection of a Mo *per si*, water was also injected. To test off-target effects we injected a standard Mo (that targets a human beta-globin intron mutation that causes beta-thalessemia). p53 Mo was co-injected with *cdkn2b* Mo in order to diminish off-target effects, and p53 Mo was injected by itself to control the effect of this morpholino. The concentration used for p53 was 1.5xng of *cdkn2b* Mo used. We chose this amount of p53 Mo based on the work of Mara E. Robu et al(2007) [69]. Amount of each morpholino injected in the final studies are described in Table 4.2.

To analyze phenotypes and control the efficiency of the knockdown, some of the 24hpf embryos injected were fixed with PFA 4% and Immunohistochemistry was performed (following the same protocol described in section 4.3.).

4.4.2. Rescue of phenotype by mRNA Injection

In order to rescue the *cdkn2b* Mo obtained phenotype, *cdkn2b* mRNA was also injected with *cdkn2b* Mo. The RNA used in the rescue was obtained using 1µg of the DNA hydrolised with BamH I [the same from the synthesis of the probe (section 4.2.1.)] using the mMESSAGE *mMACHINE* Kit (Life Technologies, Carlsbad, California) and T3 DNA Polymerase. After running a sample of the RNA in a 0.8% agarose gel, RNA was quantified using nanodrop and stored at -80ºC.

To find the right concentration of mRNA to rescue our phenotype we start by co-injecting different concentrations of *cdkn2b* mRNA (0.01ng, 0.02ng, 0.03ng, 0.04ng, 0.07ng, 0.08ng, 0.09ng and 0.10ng) with *cdkn2b* Mo (2.4ng).

Table 4.1. – Sequences of the morpholinos used

Morpholino	Sequence
cdkn2b-Mo	5’ TCAGTTCATCCTCGACGTTCATCAT3’
cdkn2b-Mo2	5’TCGCTTCACAGGTAAAACCAAATGA 3’
p53-Mo	5’ GCGCCATTGCTTTGCAAGAATTG 3’
Standard-Mo	5’ CCTCTTACCTCAGTTACAATTTATA 3’

Table 4.2. – Final amount of solution of morpholinos injected

Content of solution injected	ng injected
cdkn2b-Mo	2.4
cdkn2b-Mo2	12.0
cdkn2b-Mo + cdkn2b-Mo2	1.7+8.4
cdkn2b-Mo + p53-Mo	2.4+3.6
Standard-Mo	2.4
p53-Mo	3.6
cdkn2b-Mo + RNA cdkn2b	2.4+0.09
cdkn2b-Mo + RNA cdkn2b	2.4+ 0.1

4.4.3 Imaging

Embryos were photographed using a slide with a Leica Z6APO stereoscope equipped with a Leica DFC490 digital camera and pictures were produced using Adobe Photoshop and Illustrator. In order to image the vessels marked with GFP from *fli1a:EGFP* zebrafish the embryos were mounted in the same manner as described before and the imaging was performed using a confocal point-scanning microscope (LSM710; Carl Zeiss), using a 10x dry objective. The pictures were analyzed using Fiji (ImageJ NIH) and Adobe Photoshop and Illustrator.

4.5 Statistics

Statistical significance ($p<0,05$) of the phenotype obtained among morphant groups and the control not injected was determined by Wilcoxon signed-rank test. This test was performed using the program RStudio.

Chapter 5: **Results**

5.1 Expression of *cdkn2b* during zebrafish development

5.1.1 mRNA expression of *cdkn2b*

Studies on the *cdkn2b* gene expression have never been performed in zebrafish embryos and the importance of the gene it is not well known. Therefore, to understand the function of the gene in the fish, we have started by characterizing *cdkn2b* expression pattern during development. In order to do so, we have done a *whole-mount in situ* hybridization in embryos with 24hpf, 48hpf and 72hpf (Fig. 5.1). Since there were any prior indication of the expression of this gene we chose to test the time-points mostly used in bibliography.

Whole-mount *in situ* hybridization were performed in three independent times using each time 10 embryos for each time-point.

As a positive control we used *sox9b*, whose expression is at brain ventricular zone and branchial arches (arrows, Fig. 5.1A). The expression of *sox9b* was consistent with the data presented in Zfin (ZFIN ID: ZDB-PUB-040907-1) giving us indication that there was no problem with the protocol used.

In order to observe the non-specific integrations of our antisense probe, we used a sense probe as a negative control, which was the complementary sequence of our antisense probe. No relevant staining was observed in the negative control (Fig. 5.1 C,E,G), pointing to the specificity of the signal present when using the antisense probe.

As results of the *in situ* hybridization, we could observe that *cdkn2b* was expressed not only in the midbrain and the hindbrain but also in the cephalic mesoderm of fish at 24hpf (Fig. 5.1B, D). Later, at 48hpf and 72hpf, *cdkn2b* was expressed in the cephalic region of the fish, although its exact location was not clear (Fig. 5.1F,H). To answer this question it is going to be necessary to do an *in situ* hybridization in sections of the cephalic region of the fish (discussed in detail in chapter 6).

At 24hpf and 48hpf, it is visible a light staining all over the fish. Nonetheless, it was not clear from our results, whether there is a weak expression or background staining.

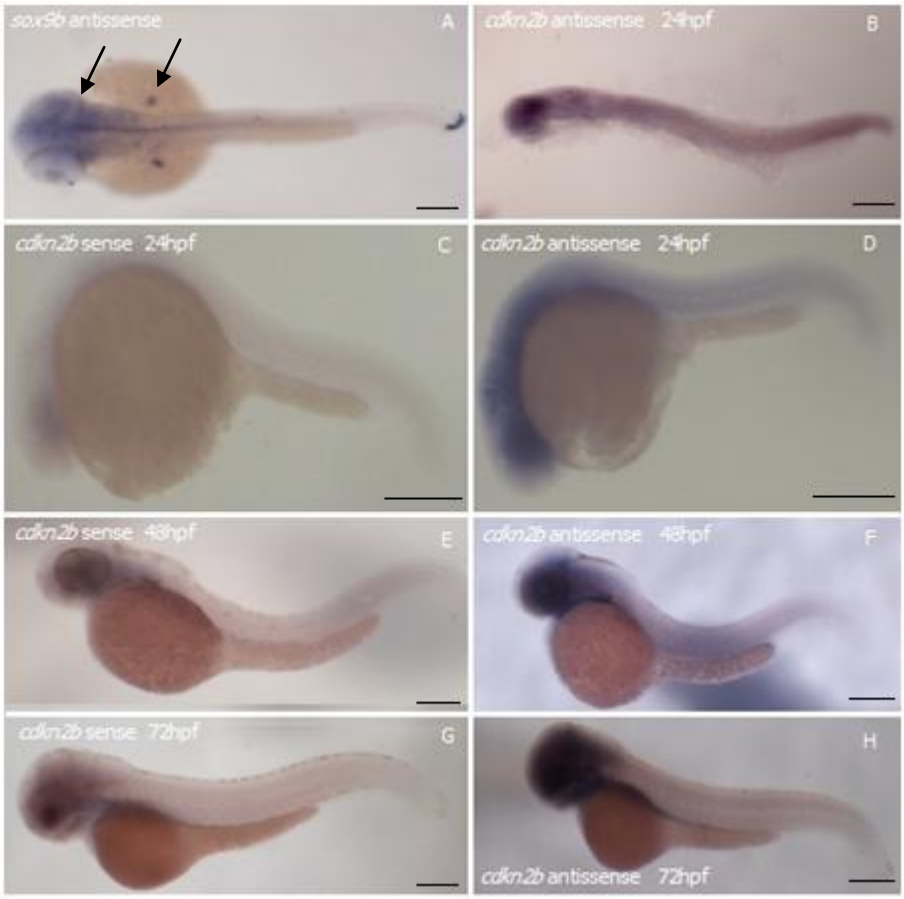

Figure 5.1 - Expression of *cdkn2b* gene in zebrafish *wt* AB embryos. Whole-mount *in situ* hybridization using gene specific digoxigenin-labeled RNA in embryos staged at 24hpf (B, C, D), 48hpf (A,E,F) and 72hpf (G, H). Dorsal view (A, B) and Lateral view (C-H). Expression pattern of *cdkn2b* (B, D, F, H) (n=10 in three independent experiments). Positive control: expression pattern of *sox9b* (A). Negative control: expression pattern obtained from a sense probe of *cdkn2b* (C,E,G). Pictures were taken using a magnifying glass. Scale bars: 200μm.

5.1.2 Protein expression of *cdkn2b*

Besides the characterization of *cdkn2b* expression using *whole-mount in situ* hybridization, it is also important to characterize where the protein is being expressed. This can be important to discover the function of *cdkn2b*, but also can give us a clue about possible regulation at the translation level. To do this characterization we used Immunohistochemistry using rat anti-cdkn2b antibody in embryos with 24hpf, 48hpf and 72hpf of development (Figs. 5.2 and 5.3).

Immunohistochemistry results were performed in three independent experiments using in each time-point 3 embryos analyzed.

In order to perceive if the signal obtained was specific from our protein, several negative controls were used (Fig. 5.2). Signal observed without primary antibody was located

especially in the yolk of the fish, and it was very faint, showing that there was not a relevant non-specific binding of secondary antibody (Fig. 5.2 A-F). Signal observed using primary but not secondary antibody was also very faint at all time-points analyzed (Fig. 5.2 G-L) only allowing to detect autofluorescence of the primary antibody and the tissue.

With these results, we were more confident that specific signal of cdkn2b expression is being detected.

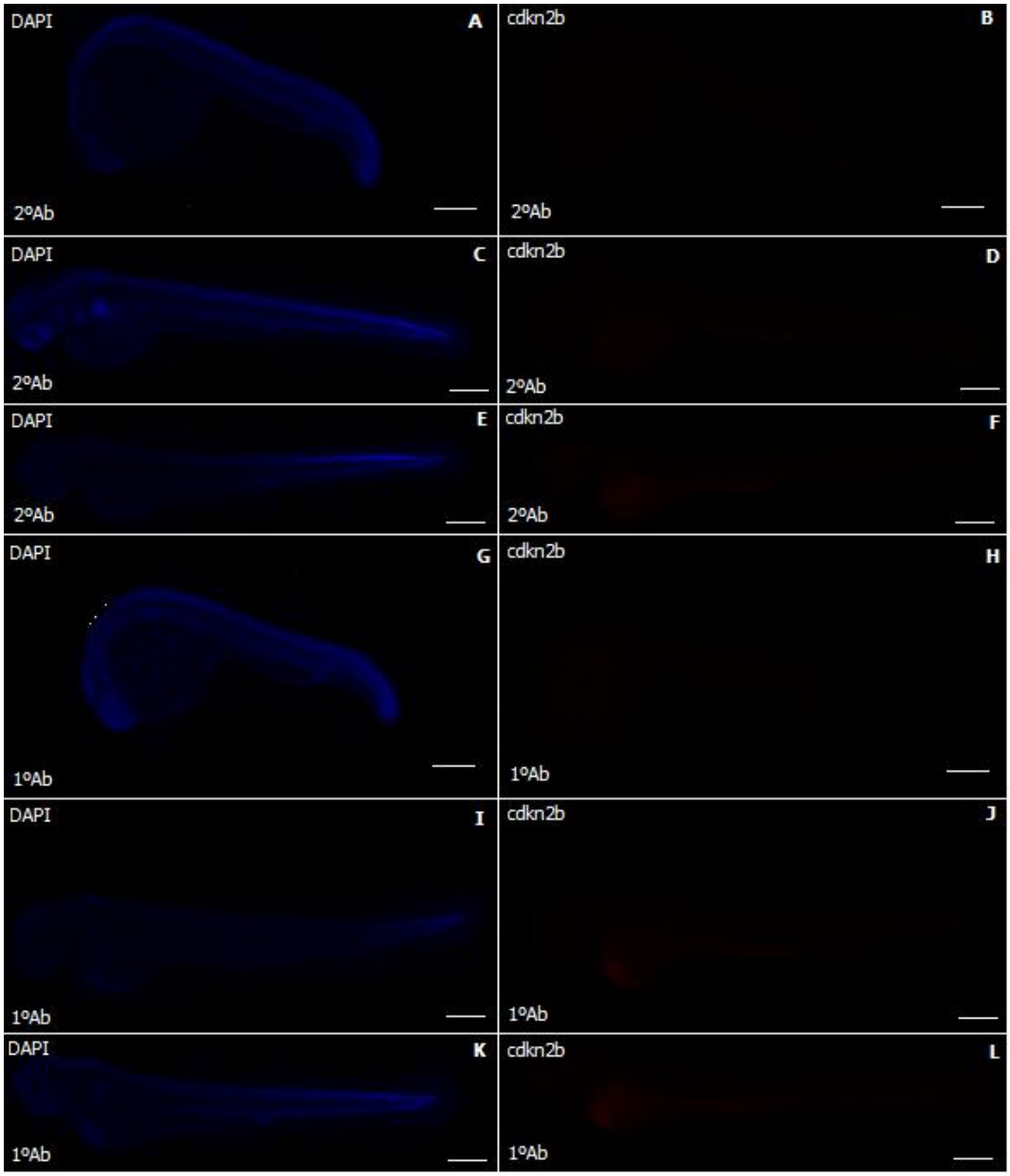

Figure 5.2 – Negative controls for Immunohistochemistry performed in zebrafish embryos with 24hpf (A, B, G, H), 48hpf (C, D, I, J) and 72hpf (E, F, K, L) for detection of cdkn2b protein expression. Lateral view (A-L). DAPI (A, C, E) and cdkn2b (B, D, F) detection results for immunohistochemistry performed without using primary antibody, but only secondary antibody Alexa Fluor 568 anti-rat. DAPI (G, I, K) and cdkn2b (H, J, L) detection results for immunohistochemistry performed using only the primary antibody, rat anti-Ink4b, but without secondary antibody. These results are representative figures of an experiment performed in three embryos in three independent time-points. Scale bar: 200μm.

From our characterization of cdkn2b expression we conclude that it is being expressed in the epidermis of the fish. At all time-points analyzed, cdkn2b have a widespread expression in the fish at the level of epidermis. Comparing DAPI and cdkn2b expression, protein seems to be expressed more specifically in the cytoplasm of the cells (white arrows in Fig. 5.3H,K).

Although the existence of this widespread pattern of expression in the fish, it came to our attention that expression of cdkn2b forms a strange pattern of in the epidermis with spaces without expression (yellow arrows, Fig.5.3K). This strange pattern was visible especially at 48hpf and 72hpf (Fig. 5.3H,K,N).

We believe that a possible explanation for this observation could be related with cell death at the moment of fixation (but further discussion will be developed in chapter 6).

It is also visible some “round gaps” in between the cells expressing cdkn2b, but this gaps are normal in the epidermis of the fish (blue arrows in Fig. 5.3H,K,N).

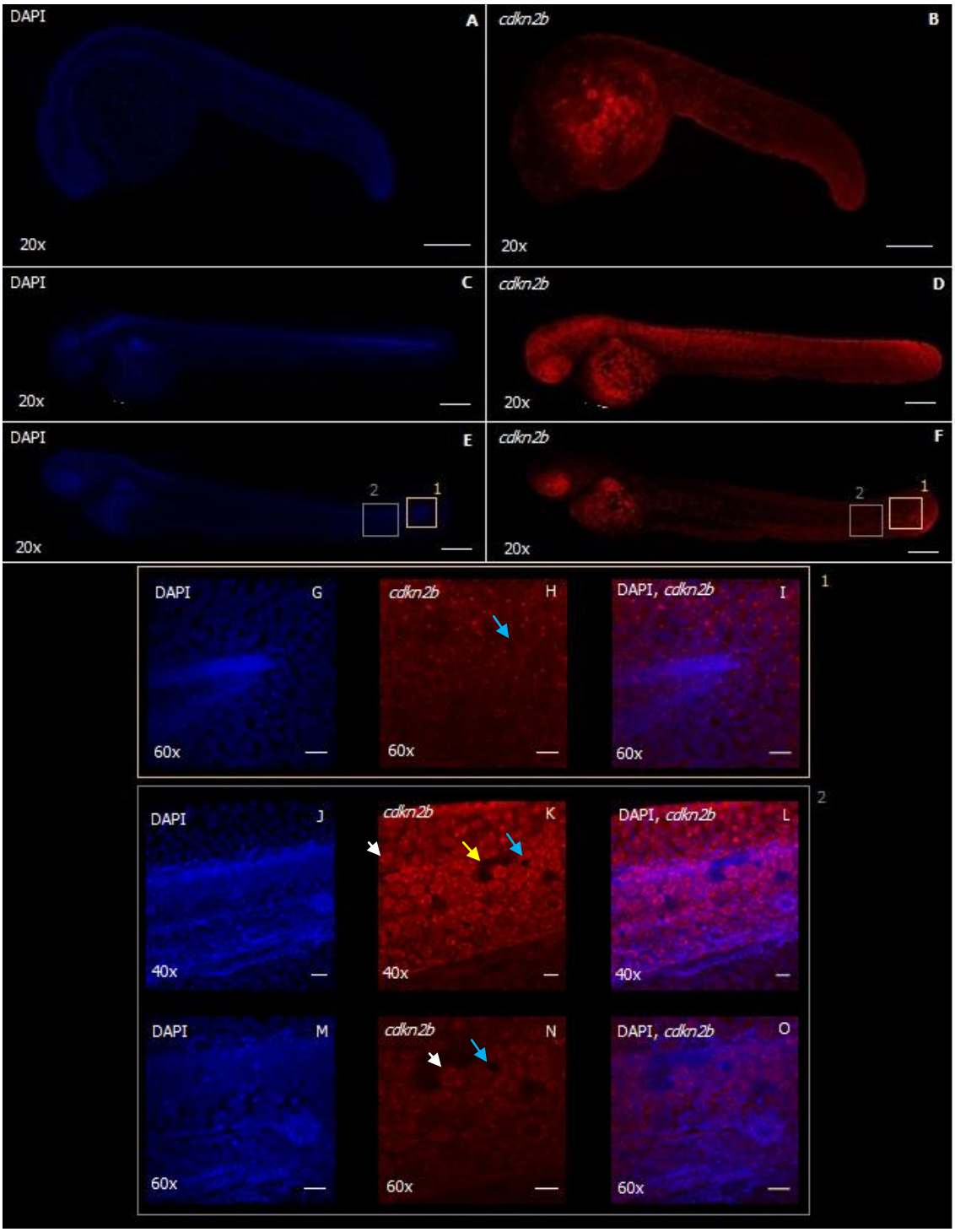

Figure 5.3 – Expression of cdkn2b protein in zebrafish embryos at 24hpf (A,B), 48hpf(C,D) and 72hpf(E,F) detected by Immunohistochemistry using rat anti-Ink4b (primary antibody) and Alexa Fluor 568 anti-rat (secondary antibody). Lateral view (A-F). Zoom of specific parts of the fish at 72hpf (G-O). Detection of DAPI (G, J, M), cdkn2b protein expression (H, K, N), and co-localization of DAPI and cdkn2b (I, L, O). [1] Detection of signal in a more proximal region of the tip of the tail (G-I). [2] Detection of signal in a more middle region of the tail. (J-O) using 40x (J-L) or 60x (M-O) magnifications. White arrow indicate expression of cdkn2b in the cytoplasm of the cell (K, N), yellow arrow indicates a location in the epidermis of the fish where there is no expression of cdkn2b (K), blue arrow indicates a "round gap" usually present in the epidermis(H, K, N). These results are representative figures of an experiment performed in three embryos in three independent time-points. Scale bar: 200μm (A-F). Scale bar 20μm (G-O).

5.2 Development of zebrafish embryos in absence of *cdkn2b*

5.2.1 Influence of *cdkn2b* in correct body axis and tail formation during zebrafish development

In order to understand if changes in *cdkn2b* gene expression produce phenotypic effects in zebrafish embryos during the early stages of development we used microinjection of antisense morpholino oligonucleotides (Mos) into the yolk of one-cell stage embryos. In total, 2 different translation blocking Mos were analyzed, and several controls tested (both Mos at once, standard control, injection with H_2O, co-injection with p53 Mo, p53 Mo, rescue experiments and immunohistochemistry assays).

When using Mos it is important to choose the right concentration to use. A low concentration might be unable to educe a phenotype. Excess of Mo can produce off-target effects affecting embryos mortality or inhibiting unspecific targets when injected. In the present work, we have started by testing different amounts of *cdkn2b* Mo and examining the morphology and the mortality rate of the embryos injected. We have generated a 'dose-response' curve for the morpholino, by titrating it down to a level at which it does not elicit a phenotype. Embryos were checked at regular time-points (24, 48 and 72hpf) for each injection experiment.

When injecting 1.2ng and 1.8ng of *cdkn2b* Mo, the embryos were like the control not injected at all time-points. When injecting 2.4ng or 3.6ng of the morpholino, some of the embryos showed heart edema, neural death, and most of the embryos showed curly-body axis and a deformed tail. All the embryos with a turned tail also showed a curly-down body axis. On one hand, the turned tail was the most consistent alteration observed. On the other hand, heart edema and neural death are known to be frequent side effects when using Mos. So we have considered a phenotype when a 72hpf embryo had a turned tail and a curly-down body axis (Fig 5.7). We choose to considerer the phenotype at 72hpf because this was the last time-point checked, and at this point there was no dough about presence or absence of phenotype.

The average of embryo lethality for all the experiments and the presence of a phenotype was converted to a percentage and plotted on graphs for all the different concentrations of morpholino used (fig. 5.4).

In the following experiments we choose to use the lower concentration that caused a phenotype (2.4ng of *cdkn2b* Mo). We choose this concentration because embryos showed less side effects then embryos injected with 3.6ng, the mortality rate was substantially lower than mortality rate when injecting 3.6ng and this allowed us to use less of our morpholino stock

solution. Although the mortality rate of the embryos injected with 2.4ng is lower than embryos injected with 3.6ng, it is substantially higher than mortality rate of the embryos not injected (fig 5.4D).

This is caused, not only because of the secondary effects of the morpholino, but also because of the microinjection technique by *per si*.

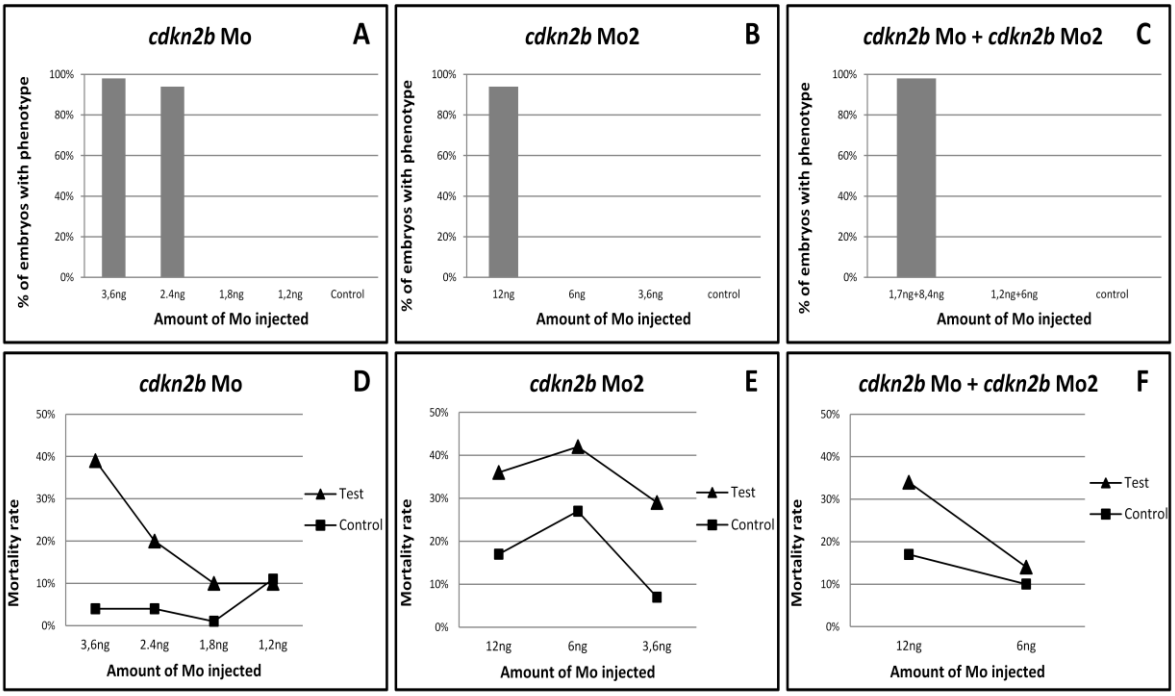

Figure 5.4- Effect of injection of different concentrations of morpholinos against *cdkn2b* in *wt* AB zebrafish embryos. Percentage of embryos with phenotype at 72hpf (A-C) observed when injecting different concentrations of *cdkn2b* Mo (A), *cdkn2b* Mo2 (B) or *cdkn2b* Mo + *cdkn2b* Mo2 (C). Mortality rate of embryos at 24hpf observed when injecting different concentrations of *cdkn2b* Mo (D), *cdkn2b* Mo2 (E) or *cdkn2b* Mo + *cdkn2b* Mo2 (F). Phenotypes and mortality rates of injected embryos were compared with non injected embryos (control).

A morpholino has approximately 25% chance of having off-target phenotypes. The chance of two Mos yielding the same off-target phenotypes is considerably low. In order to gain more confidence on our results we designed a second, non overlapping *cdkn2b* Mo (*cdkn2b* Mo2) against the gene of interest to see if the phenotypes obtained were similar. The second morpholino was also a translation-blocking morpholino. With the same purpose has before, we also generated a 'dose-response' curve for Mo2 (Fig. 5.4B,E). Once again, the lower concentration causing a phenotype (12ng of *cdkn2b* Mo2) was chosen.

The different amount of morpholinos (2.4 ng *cdkn2b Mo* and 12 ng *cdkn2b* Mo2) needed to cause the same phenotype can be explained by the different 'penetrances' of the morpholinos. *cdkn2b* Mo seems to have a higher penetrance than *cdkn2b* Mo2, so a lower concentration of *cdkn2b* Mo was needed to cause the same phenotype. Nevertheless,

embryos injected with *cdkn2b* Mo or *cdkn2b* Mo2 presented the same phenotype, embryos with a turned tail and a curly-down body axis at 72hpf.

Besides testing the two morpholinos isolated, more confidence can be gained by injecting the two Mos together at a level that does not elicit phenotypes on their own. As it was done for the Mos separately, we also generated a 'dose-response' curve for *cdkn2b* Mo and *cdkn2b* Mo2 when being injected together (*cdkn2b* Mo+*cdkn2b* Mo2) (Fig. 5.4C,F). In this case, we chose to use 1.7ng of *cdkn2b* Mo and 8.4ng of *cdkn2b* Mo2 for the same reason previously referred for the other Mos. Once again, embryos presented a curly-down body axis and a turned tail at 72hpf.

In conclusion, injecting *cdkn2b* Mo, *cdkn2b* Mo2 or *cdkn2b* Mo+*cdkn2b* Mo2 it causes the same phenotype, a turned tail and a curly-down body axis.

In addition to injecting a second morpholino, we also tested a standard control morpholino (standard Mo) available in the lab, a morpholino that affects a gene that is not expressed in the fish (targets a human beta-globin intron mutation that causes beta-thalessemia). This control alone is insufficient to see if the phenotype is specific or not, but helps to control the effects of the injection and some possible off-target effects. Furthermore, we have also injected embryos with only water to guarantee that the injection process was not responsible *per si* for any of the phenotypes observed.

At all time-points studied, the embryos injected with standard control and water didn´t showed phenotype differences from the embryos not injected (Figs. 5.5C, D; 5.6 C, D and 5.7C, D),

After optimizing the amount of each Mo injected and testing several controls, phenotypes obtained were analyzed in detail.

At 24hpf, embryos injected with *cdkn2b* Mo showed different levels of neural death. Neural death can be identified by highly localized opaque cells in the cephalic region of the embryo, which are in areas of the developing brain (Fig. 5.5 E,F). Knocking down of some genes using Mos can cause neural death by activation of p53. The neural death seen might be the result of p53 activation. The embryos which presented neural death also looked thinner than embryos not injected. Some of the embryos injected with *cdkn2b* Mo didn´t show relevant differences from the control not injected.

Besides neural death, at 24hpf embryos didn´t showed relevant differences from control not injected.

The morphants obtained from injecting *cdkn2b* Mo2 (Fig. 5.5G) and *cdkn2b* Mo+ *cdkn2b* Mo2 (Fig. 5.5H) only presented low level of neural death in some of the embryos and

the rest of the parts of the embryo also appears to be similar to the ones in the control not injected.

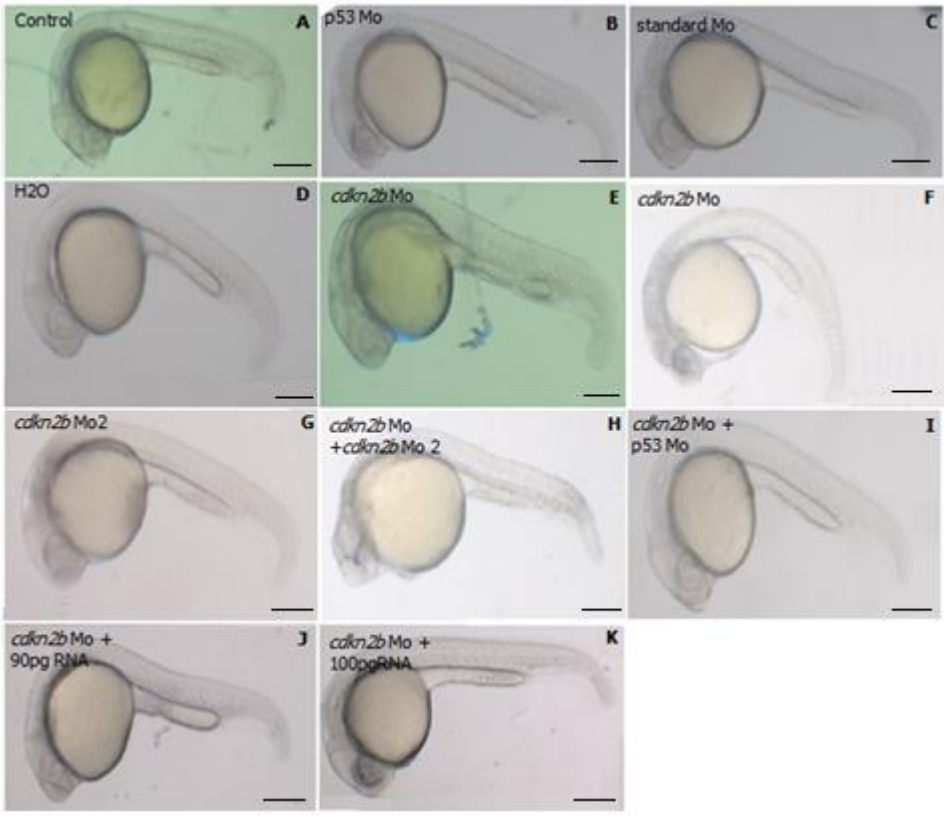

Figure 5.5 – Knockdown of *cdkn2b* in *wt AB* embryos at 24hpf using morpholino injected at one cell stage and respective controls. Lateral view of embryos: control not injected (A); injected with p53Mo (B), standard Mo (C), water (D), *cdkn2b* Mo (E, F), *cdkn2b* Mo2 (G), co-injection of *cdkn2bMo* with *cdkn2bMo2* (H), *cdkn2b* Mo with p53Mo (I), *cdkn2b* Mo with 90pg mRNA of *cdkn2b* (J) and *cdkn2b* Mo with 100pg mRNA of *cdkn2b* (K). Scale bars: 200μm.

Later in development (Figs. 5.6 and 5.7), at 48hpf and 72hpf morphants, *cdkn2b* Mo and *cdkn2b* Mo + *cdkn2b* Mo2 embryos showed a curly-down body axis with turned tails and continued showing neural death. Embryos with high levels of neural death were thinner and smaller. Morphants *cdkn2b* Mo2 were also a little curved and showed defects on the tail but at this point there weren't significant signals of neural death in the embryos. For all the morphants (*cdkn2b* Mo, *cdkn2b* Mo2 and *cdkn2b* Mo+ *cdkn2b* Mo2), the curvature present in the tail didn´t showed a regular pattern, it was slightly different from embryo to embryo.

The morphants *cdkn2b* Mo, *cdkn2b* Mo2 and *cdkn2b* Mo + *cdkn2b* Mo2 presented a phenotype prevalence of statistically different from the controls not injected $p<0.05$ for *cdkn2b* Mo and *cdkn2b* Mo2 and $p<0.01$ for *cdkn2b* Mo + *cdkn2b* Mo2 (Fig.5.8). These results support the specificity of the phenotype observed.

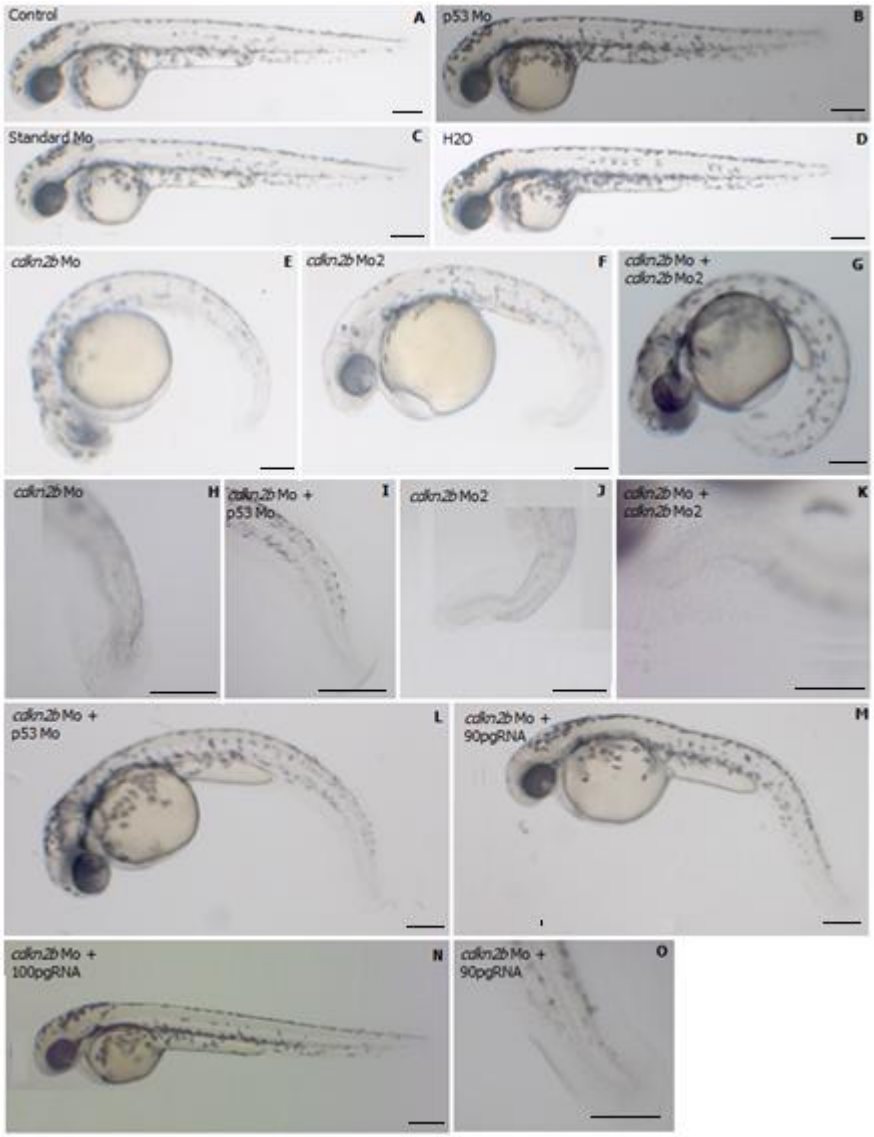

Figure 5.6 – Knockdown of *cdkn2b* in *wt AB* embryos at 48hpf using morpholino injected at one cell stage and respective controls. Lateral view of embryos: control not injected (A); injected with p53Mo (B), standard Mo (C), water (D), *cdkn2b* Mo (E), *cdkn2b* Mo2 (F), co-injection of *cdkn2bMo* with *cdkn2bMo2* (G), *cdkn2b* Mo with p53Mo (L), *cdkn2b* Mo with 90pg mRNA of *cdkn2b* (M) and *cdkn2b* Mo with 100pg mRNA of *cdkn2b* (N). Zoom of the tail of the embryos injected with *cdkn2b* Mo (H), *cdkn2b* Mo2 (J), co-injection of *cdkn2b* Mo with p53Mo (I), *cdkn2b Mo* with *cdkn2b* Mo2 (K), or *cdkn2b* Mo with 90pg mRNA of *cdkn2b* (O). Scale Bar: 200μm.

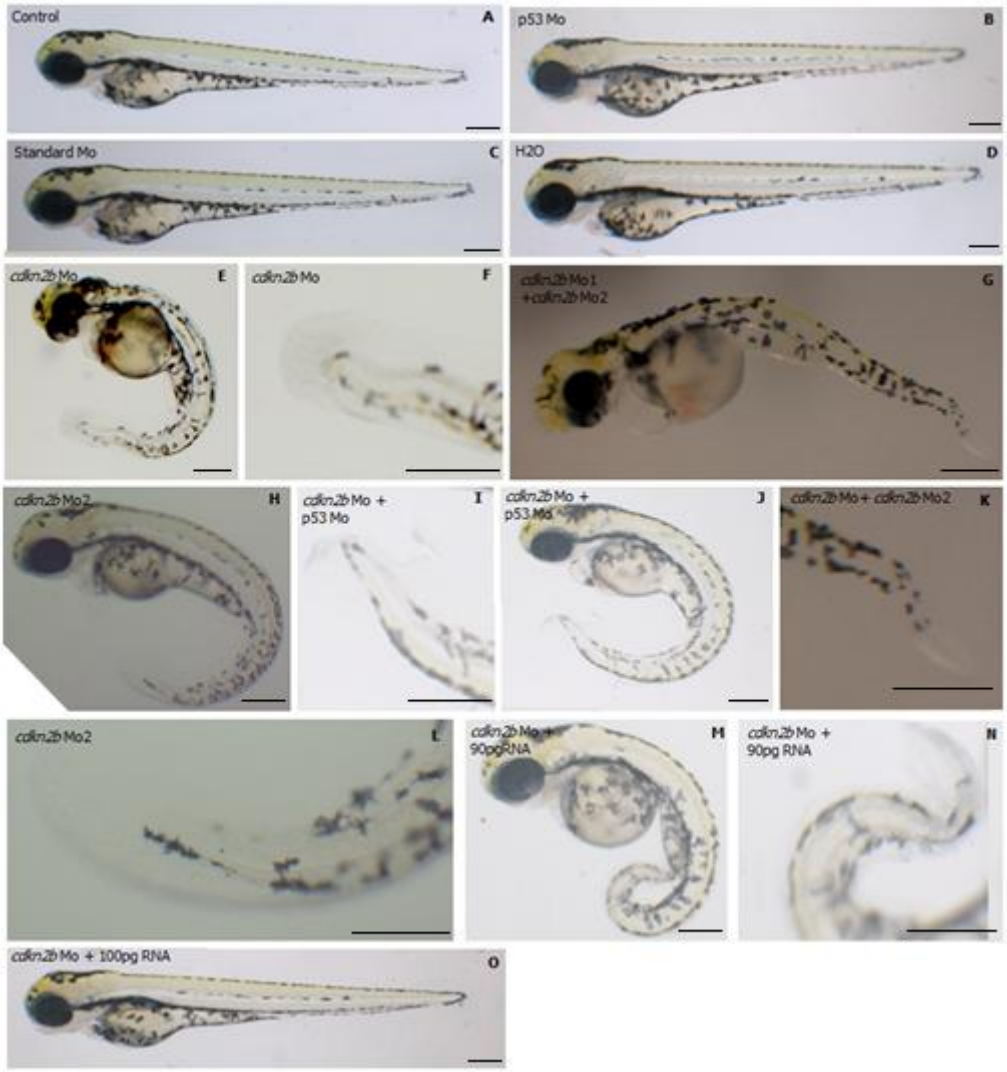

Figure 5.7 - Knockdown of *cdkn2b* in *wt* AB embryos at 72hpf using morpholino injected at one cell stage and respective controls. Lateral view of embryos: control not injected (A); injected with p53Mo (B), standard Mo (C), water (D), *cdkn2b* Mo (E,F), *cdkn2b* Mo2 (H, L), co-injection of *cdkn2b* Mo with *cdkn2b* Mo2 (G,K), *cdkn2b* Mo with p53Mo (I,J), *cdkn2b* Mo with 90pg mRNA of *cdkn2b* (M, N) and *cdkn2b* Mo with 100pg mRNA of *cdkn2b* (O). Zoom of the tail of embryos injected with *cdkn2b* Mo (F), *cdkn2b* Mo2 (L), co-injection of *cdkn2bMo* with *cdkn2bMo2* (K), *cdkn2b* Mo with p53Mo (I), *cdkn2b* Mo with 90pg mRNA of *cdkn2b* (N). Scale bar: 200µm.

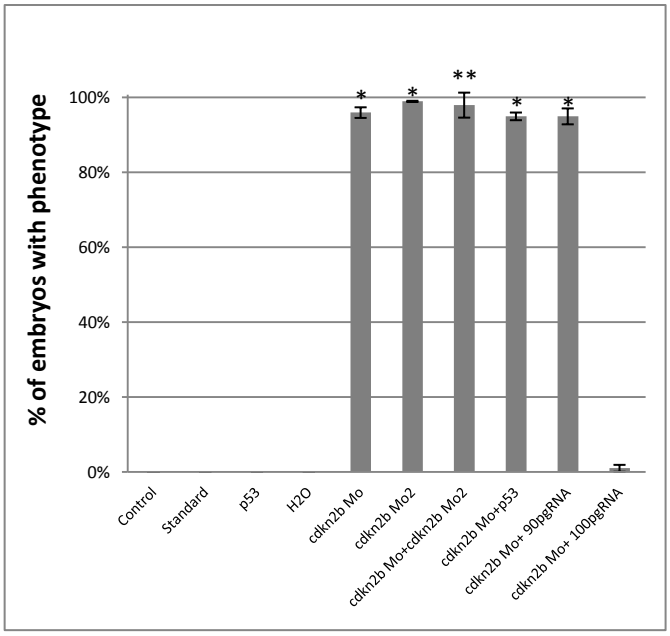

Figure 5.8 - Percentage of *wt* AB zebrafish embryos presenting phenotype at 72hpf when injected with different morpholinos against *cdkn2b* (*cdkn2b* Mo, *cdkn2b* Mo2, *cdkn2b* Mo+ *cdkn2b* Mo2) and respective controls (control – not injected, standard Mo, p53Mo, H_2O, *cdkn2b* Mo + 90pg mRNA, *cdkn2b* Mo + 100pg mRNA). The bars are repsesentative of the standard derivation. Statistical differences between morphants group and the control not injected for * $p<0.05$ or ** $p< 0.01$.

To test if the neural death observed was the result of p53 activation we co-injected *cdkn2b* Mo with p53 Mo. Since the second morpholino was injected with a higher concentration than *cdkn2b* Mo, and *cdkn2b* Mo2 showed low levels of neural death, we only co-injected p53Mo with the *cdkn2b* Mo. Embryos injected with p53Mo isolated were, at all time-points, similar to the controls not injected (Fig.5.5B, 5.6B and 5.7B).

When injected in combination (*cdkn2b* Mo with p53 Mo), the neural death caused by *cdkn2b* Mo was attenuated by p53 co-knockdown. At all time-points, we had less neural death. Although there weren´t significant differences from the control not injected at 24hpf, the embryos continued to have defects on the tail at 48hpf and 72hpf with a statistical significance higher than 97%. The phenotype observed was similar to the obtained in embryos injected with *cdkn2b* Mo2, reinforcing the idea that *cdkn2b* is responsible for the phenotype observed in the tail and the curly-down body axis of the fish and that neural death could be the result of off-targed effects of the morpholino.

All the controls referred before were important to analyze if the phenotype was specific from the morpholino. Nonetheless they don't give us information about the morpholino effectiveness. Since we used translation-blocking morpholinos, we wanted to confirm *cdkn2b* knockdown. In this sense, after injecting embryos in one-cell stage we fixed embryos at 24hpf. Then, we did a Immunohistochemistry and compared the outcome with the

Immunohistochemistry results presented before (section 5.1.2). These control experiments were performed in three independent times. In each time we have analyzed three embryos injected with each of the Mos, *cdkn2b* Mo and *cdkn2b* Mo2.

In all the embryos analyzed, it was not detected signal of cdkn2b, proving the effectiveness of *cdkn2b* knockdown.

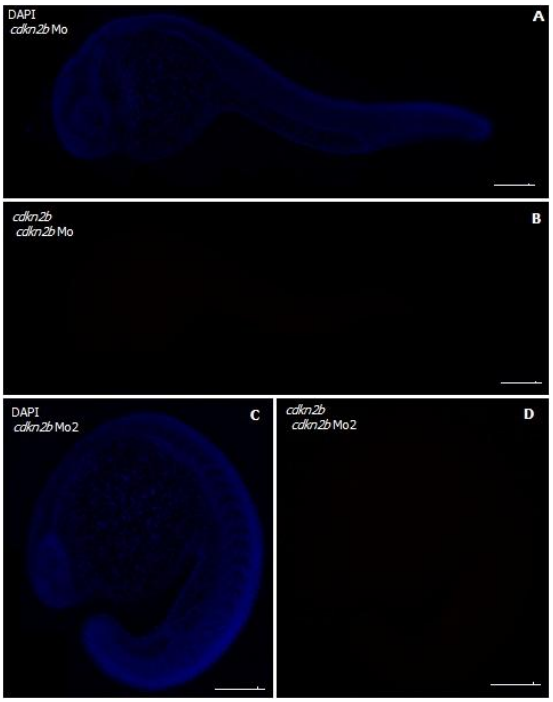

Figure 5.9 – Immunohistochemistry results from *cdkn2b* knockdown embryos at 24hpf by injection of *cdkn2b* Mo and *cdkn2b* Mo2. Lateral view of zebrafish embryos. DAPI expression in zebrafish embryos at 24hpf after injecting at one-cell stage *cdkn2b* Mo (A) and *cdkn2b* Mo2 (C).Expression of cdkn2b protein in zebrafish embryos at 24hpf after injecting at one-cell stage *cdkn2b* Mo (B) and *cdkn2b* Mo2 (D). The embryos presented in this figure are representative of three independent experiments performed in three embryos each. Scale bar: 200μm.

Nevertheless, a direct relation between *cdkn2b* and the curved tail and a curly-down body axis phenotype obtained still needs to be further elucidated.

Although some confidence can be gained by all the controls performed before, we opted also by doing a rescue of the phenotype. This was really important to test the specificity of our morpholino. In this sense, different amounts of *cdkn2b* mRNA were injected in *wt* AB embryos in combination with *cdkn2b* Mo solution to see if the phenotype disappeared. The mRNA injected had exactly the same sequence as the mRNA from *cdkn2b* listed in detail in Zfin.

Once again, we generated a 'dose-response' curve for mRNA to see the amount of mRNA necessary to rescue the phenotype (Fig. 5.10) without the possible secondary effects resulting from over expression of the protein, or expression of the protein in unusual tissues.

At 24hpf, the embryos injected with 90pg of *cdkn2b* mRNA were similar to the control not injected. At 48hpf and 72hpf, the tails of the embryos continued to be turned. The phenotype observed was similar to the phenotype of embryos injected with *cdkn2b* Mo +p53 Mo. This may be the result from reducing the concentration of free *cdkn2b* Mo. When injecting 100pg, at all time-points analyzed, the embryos looked similar to the controls not injected.

This recovery of the well development of the tail indicates that turned tail and the curly-down body axis might be a phenotype resulting from the knockdown of *cdkn2b*.

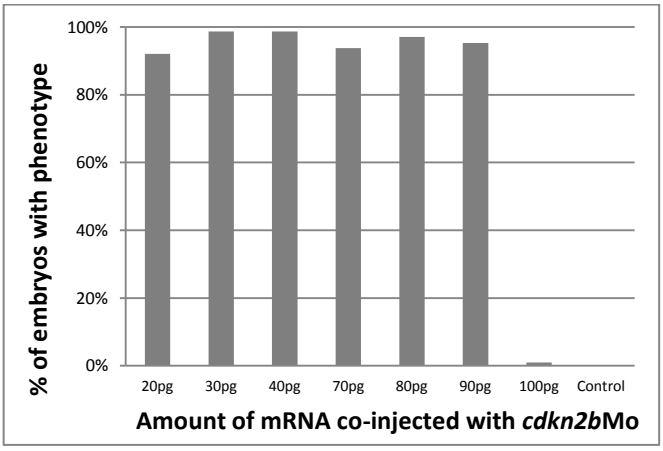

Figure 5.10 - Assays performed to rescue phenotype caused by *cdkn2b* knockdown using morpholinos. Percentage of *wt* AB zebrafish embryos presenting phenotype at 72hpf when co-injecting *cdkn2bMo* and different concentrations of *cdkn2b* mRNA. In the X axis we can see the amount of *cdkn2b* mRNA co-injected with 2.4ng of *cdkn2b* Mo per embryo. Since all the controls not injected had the same percentage of embryos with phenotype, "Control" represent all the embryos not injected in all the experiments.

5.2.2 Vessel formation in the absence of *cdkn2b* during Zebrafish development

Besides characterizing *cdkn2b* in zebrafish embryos, another aim of the project was to understand if *cdkn2b* is involved in the formation of the vessels of the fish. Therefore, we wanted to identify if there were any difference in the vessels morphology after knocking down *cdkn2b*. In this sense, after injecting *cdkn2b* Mo and *cdkn2b* Mo2 in *wt* AB embryos we have also injected embryos resulting from crossing *fli1a:EGFP* heterozygous male and a *wt AB* female. In this way, we could analyze in parallel the *fli1a:EGFP* and its siblings *wt* AB. When injecting these embryos, we obtained exactly the same phenotype in all of the embryos, and this phenotype was consistent with the one obtained when crossing only *wt AB.*

All the embryos used after this moment were the result of crossing *fli1a:EGFP* heterozygous with *wt* AB, and the *fli1a:EGFP* embryos were selected at 24hpf using a fluorescence magnifier. The embryos phenotype was analyzed using a fluorescence magnifier

and then photographed using a confocal point-scanning microscope (ampliations 10x). The morpholinos injected and the time-points analyzed were the same as described before (Figs. 5.11, 5.12 and 5.13).

At 24hpf, injection of *cdkn2b* Mo by itself (Fig. 5.11 B,E) resulted in morphants with a caudal vein (cv) slightly deformed at the tail of the fish when compared to the non injected controls. This phenotype was also observe in the *cdkn2b* Mo2 and *cdkn2b* Mo+ *cdkn2b* Mo2 morphants (Fig. 5.11 C,F,G,J). When injecting *cdkn2b* Mo +p53M (Fig. 5.11 H,K), morphants also presented alterations in the caudal vein, namely an enlarged/more dense vein. According to these results, we believe that the cv phenotype is specific from the *cdkn2b* knockdown.

When injecting 90pg of mRNA the embryos still presented alterations in the caudal vein. Furthermore, when we did the rescue with 100pg of mRNA (Fig. 5.11 M,N), the embryos looked the same as the controls not injected (Fig. 5.11 A,D), recovering the caudal vein phenotype of the controls. These data, reinforces the idea that *cdkn2b* could have an important role in the tail/vessel formation.

Later in development, 48hpf and 72hpf morphants (Figs. 5.12 and 5.13) injected with *cdkn2b* Mo, *cdkn2b* Mo2 or *cdkn2b* Mo + *cdkn2b* Mo2 have shown deformed tails with problems on the intersegmental vessels (Se), caudal vein (cv) and caudal artery (CA) when compared to the controls. The regular pattern of the Se was disorganized and de cv and CA looked distorted. When co-injected *cdkn2b* Mo +p53Mo, morphants presented normal Se and CA but had an enlarged tail with deformed cv and entangled vessels. Embryos injected with *cdkn2b* Mo+90pg RNA hasn't shown relevant differences from the control from the point of view of vessels morphology and injection with 100pg of RNA, completely confirmed the rescue, e.g., embryos were similar to the controls not injected (Figs. 5.12 and 5.13).

Since morphants *cdkn2b* Mo +p53Mo show normal CA and Se we considered a phenotype the presence of deformations on the cv of the fish at 72hpf. The morphants injected with *cdkn2b* Mo, *cdkn2b* Mo2 showed a phenotype in 97% of the embryos and *cdkn2b* Mo + *cdkn2b* Mo2 morphants showed phenotype in 95% of the embryos. Morphants *cdkn2b* Mo, *cdkn2b* Mo2 and *cdkn2b* Mo + *cdkn2b* Mo2 presented a phenotype prevalence of statistically different from the controls not injected $p<0.05$ for *cdkn2b* Mo and *cdkn2b* Mo2 and $p<0.01$ for *cdkn2b* Mo + *cdkn2b* Mo2 (Fig.5.8). These results support the specificity of the phenotype observed (Fig. 5.14).

In global, our results reinforce the idea that *cdkn2b* is responsible for the caudal vein but not for the Se and CA phenotypes observed at the tail of the fish.

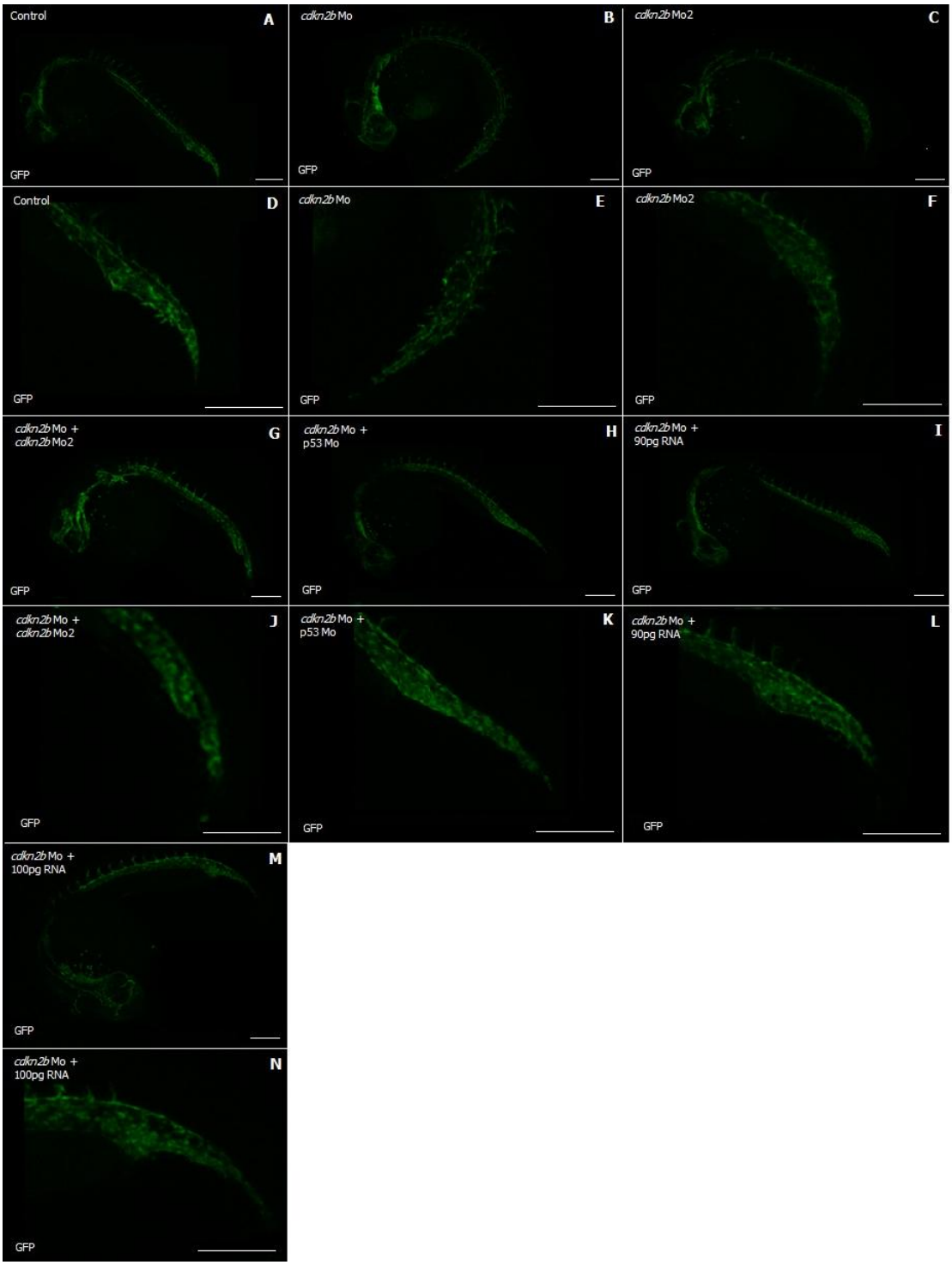

Figure 5.11- Visualization of blood vessels of transgenic *fli1a:EGFP* zebrafish in the absence of *cdkn2b* expression by knocking down with morpholinos and respective controls. Representative figures of lateral view of blood vessels from embryos with 24hpf marked with GFP not injected (A,D), injected with *cdkn2b* Mo (B,E), *cdkn2b* Mo2 (C,F), co-injected with *cdkn2bMo* and *cdkn2bMo2* (G,J), *cdkn2b* Mo and p53Mo (H,K), *cdkn2b* Mo with 90pg mRNA of *cdkn2b* (I,L) and *cdkn2b* Mo with 100pg mRNA of *cdkn2b* (M,N). Zoom of the blood vessels present in the tail of embryos not injected (D), injected with *cdkn2b* Mo (E), *cdkn2b* Mo2 (F), co-injected with *cdkn2b* Mo and *cdkn2b* Mo2 (J), *cdkn2b* Mo and p53Mo (K), *cdkn2b* Mo with 90pg mRNA of *cdkn2b* (L) or injected with *cdkn2b* Mo with 100pg mRNA of *cdkn2b* (N). Scale bar: 200µm.

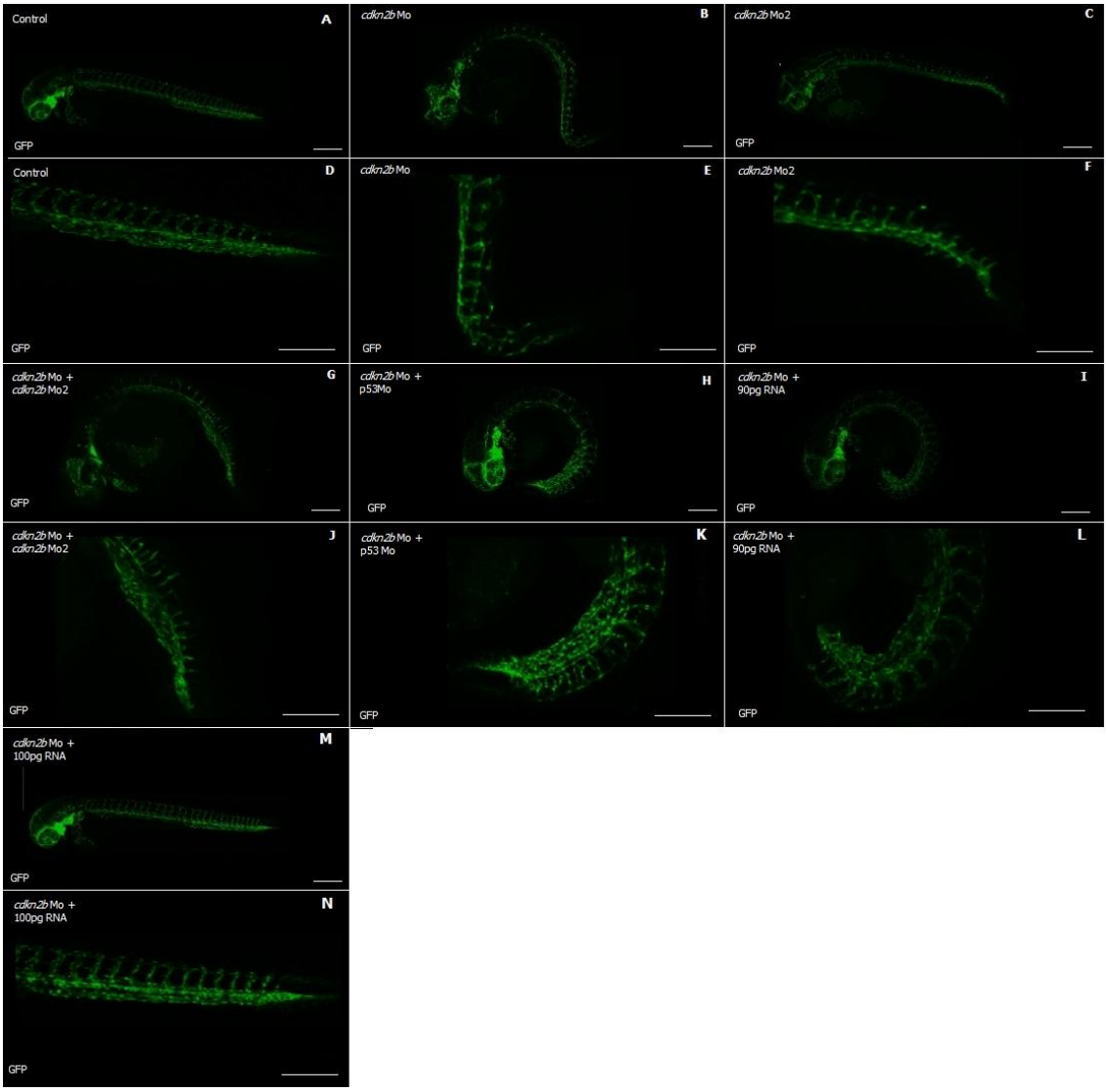

Figure 5.12- Visualization of blood vessels of transgenic *fli1a:EGFP* zebrafish in the absence of *cdkn2b* expression by knocking down with morpholinos and respective controls. Representative figures of lateral view of blood vessels from embryos with 48hpf marked with GFP not injected (A,D), injected with *cdkn2b* Mo (B,E), *cdkn2b* Mo2 (C,F), co-injected with *cdkn2bMo* and *cdkn2bMo2* (G,J), *cdkn2b* Mo and p53Mo (H,K), *cdkn2b* Mo with 90pg mRNA of *cdkn2b* (I,L) or *cdkn2b* Mo with 100pg mRNA of *cdkn2b* (M,N). Zoom of the blood vessels present in the tail of embryos not injected (D), injected with *cdkn2b* Mo (E), *cdkn2b* Mo2 (F), co-injected with *cdkn2b* Mo and *cdkn2b* Mo2 (J), *cdkn2b* Mo and p53Mo (K), *cdkn2b* Mo with 90pg mRNA of *cdkn2b* (L) or injected with *cdkn2b* Mo with 100pg mRNA of *cdkn2b* (N). Scale bar: 200μm.

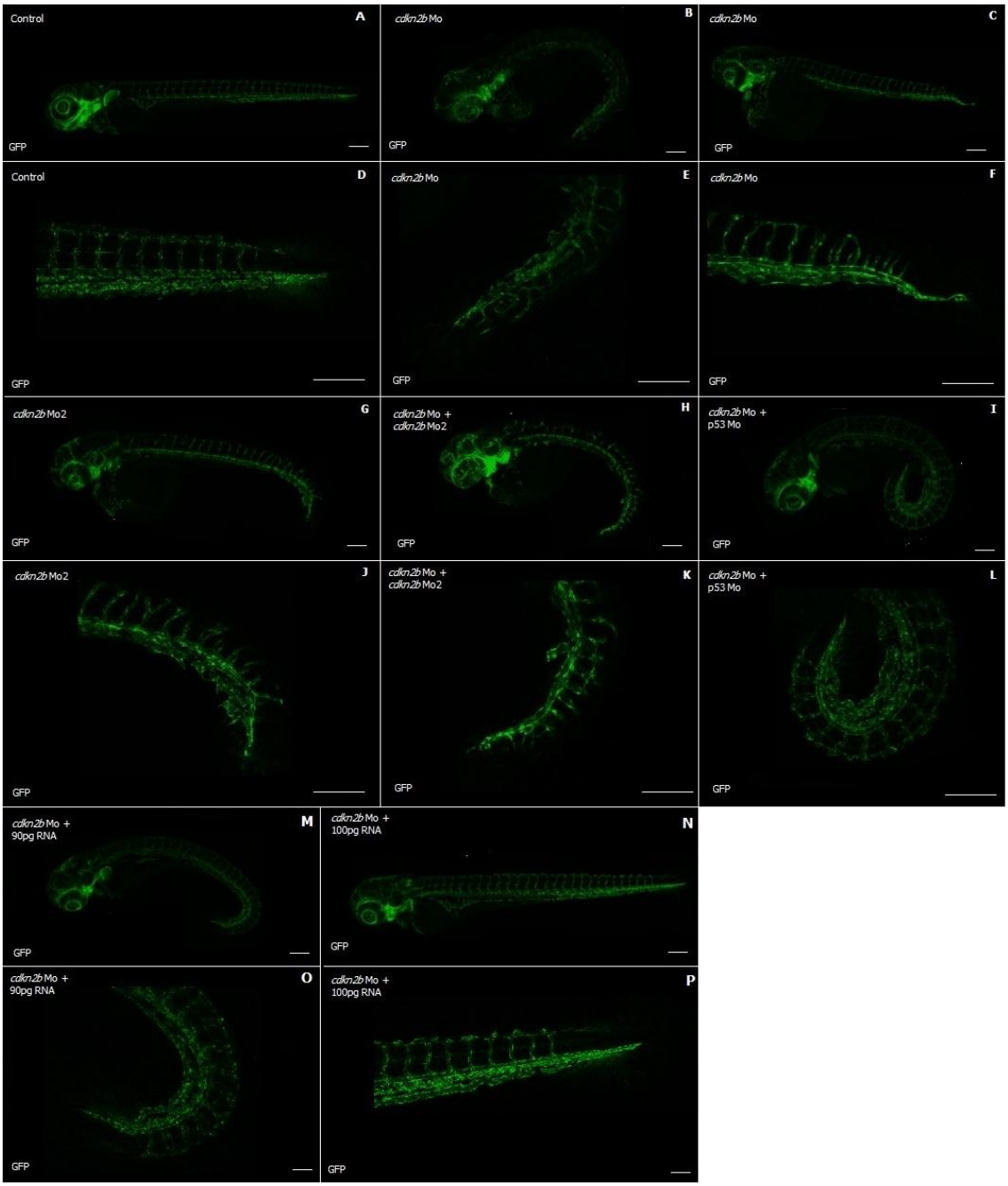

Figure 5.13- Visualization of blood vessels of transgenic *fli1a:EGFP* zebrafish in the absence of *cdkn2b* expression by knocking down with morpholinos and respective controls. Representative figures of lateral view of blood vessels from embryos with 72hpf marked with GFP not injected (A,D), injected with *cdkn2b* Mo (B,C,E,F), *cdkn2b* Mo2 (G,J), co-injected with *cdkn2b* Mo and *cdkn2b* Mo2 (H,K), *cdkn2b* Mo and p53Mo (I,L), *cdkn2b* Mo with 90pg mRNA of *cdkn2b* (M,O) and *cdkn2b* Mo with 100pg mRNA of *cdkn2b* (N,P). Zoom of the blood vessels present in the tail of embryos not injected (D), injected with *cdkn2b* Mo (E,F), *cdkn2b* Mo2 (J), co-injected with *cdkn2b* Mo and *cdkn2b* Mo2 (K), *cdkn2b* Mo and p53Mo (L), *cdkn2b* Mo with 90pg mRNA of *cdkn2b* (O) or injected with *cdkn2b* Mo with 100pg mRNA of *cdkn2b* (P). Percentage of embryos presenting phenotype at 72hpf after the injection of different morpholinos against *cdkn2b* and respective controls (Q). Scale Bars: 200μm.

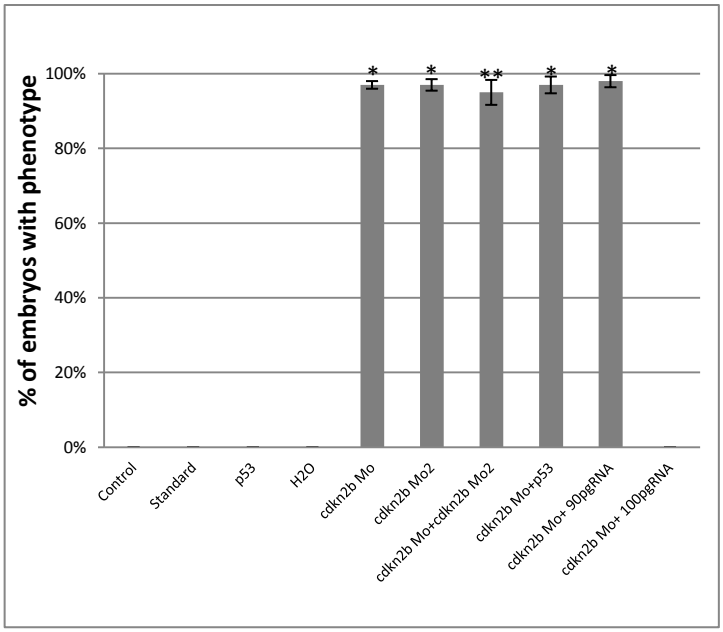

Figure 5.14 - Percentage of *fli1a:EGFP* zebrafish embryos presenting phenotype at 72hpf when injected with different morpholinos against *cdkn2b* (*cdkn2b* Mo, *cdkn2b* Mo2, *cdkn2b* Mo+ *cdkn2b* Mo2) and respective controls (control – not injected, standard Mo, p53Mo, H_2O, *cdkn2b* Mo + 90pg mRNA, *cdkn2b* Mo + 100pg mRNA). The bars are repsesentative of the standard derivation. Statistical differences between morphants group and the control not injected for * $p<0.05$ or ** $p< 0.01$.

Chapter 6: **Discussion**

CDKN2B gene encodes for one of the four known members of the INK4 family of cyclin-dependent kinase inhibitor genes, and in mammalians it is known for its role in cell proliferation, senescence, apoptosis and function as a tumor suppressor.

In zebrafish there is an ortholog of the *CDKN2B*, the *cdkn2b* gene, but until now no studies about this gene exist in zebrafish embryos. In this context, the primary objective of the present project was to characterize *cdkn2b* during zebrafish development with the purpose of finding out its function and importance.

We started the characterization of *cdkn2b* by investigating which tissues were expressing mRNA of the gene during different time-points of development (24, 48 and 72hpf) in *wt AB* embryos. For this, we choose to use *Whole-mount in situ* hybridization.

cdkn2b was mostly expressed in the cephalic region of *wt AB* embryos at all the time-points analyzed. At 24hpf it was expressed in the brain and in the cephalic mesoderm. At 48hpf and 72hpf it seems to be expressed in the cephalic region of the fish although it was slightly difficult to conclude its exact location.

The presence of *cdkn2b* expression obtained in the embryo's brain at 24hpf is in agreement with the observed in the adult zebrafish, in which the protein is known for being present in the brain, more specifically in noncycling radial glia cells, with a cytoplasmatic localization [71]. Since at 24hpf and in adult zebrafish cdkn2b appears to be expressed in the brain, at 48hpf and 72hpf the expression pattern present in the cephalic region may be specifically due to mRNA expression also in the brain.

To overcome the questions remaining about the results of the whole-mount *in situ* we are in the process of doing *in situ* hybridization in sections of the cephalic region of the embryos and in the remaining tissues of the fish.

Besides mRNA expression, it is also important to characterize cdkn2b protein expression. This can give us important information about *cdkn2b* function. Once more, since there was no previous information, we decided to do immunohistochemistry in whole embryos to detect our protein at 24hpf, 48hpf and 72hpf.

The embryos were all photographed in sections and then the staining obtained was projected. By observation of the sections and the projection, we concluded that, at all time-points analyzed, cdkn2b appears to have a widespread expression at the level of epidermis of the fish, especially at the cytoplasm of the cells. Once again, the presence of the protein in the cytoplasm is consistent with the data available from this protein in the adult zebrafish [71].

The superficial layer of the epidermis of the fish is formed by keratinocytes [56]. *In vitro* studies of keratinocytes from human (HaCat) [72] and mouse [73] it was observed that the increase of TGF-β leads to the increase of *cdkn2b* promoting cell arrest in phase G1 of cell cycle. In this sense, we believe this protein could have a role in the arrest of the cells in phase G1 of cell cycle in the epidermis of the fish.

Curiously, at 48hpf and 72hpf we have detected the absence of expression in between expressing epidermal cells, forming a peculiar pattern of cdkn2b expression.

The superficial layer of the epidermis of the embryos is formed by living cells (keratinocytes) that form a single cell layer. Cells within the epidermal layer are not periodically renewed, but are replaced individually on cell death [56,54]. This, we believe that this irregular pattern of cdkn2b expression could be related with a possible role of the protein in cell arrest, that is, absence of expression correspond to cells that were dead and that the epidermis wasn't yet able to renew at the moment of fixation.

Although we did not identified expression of *cdkn2b* mRNA in the epidermis when performing whole-mount *in situ* hybridization these results are not contradictory. The mRNA expression might be low enough not to be detected by whole-mount *in situ* hybridization. On the other hand, there can be expression of mRNA in the brain of the fish and don't exist expression of the protein. Nonetheless, more experiments would be needed in order to make a conclusion about this possible regulation.

After the characterization at mRNA and protein levels we tryed to discover the function of *cdkn2b* by blocking the translation of the protein. For this we decided to use oligo antisense morpholinos. After optimization of the quantities of the morpholino to use, it was concluded that in the absence of *cdkn2b,* the most striking phenotype was the presence of embryos with a curly-down body axis with turned tails.

According to the controls used, the confirmation of knockdown by immunohistochemistry and the rescue of the phenotype when injecting mRNA of *cdkn2b,* we believe that we have strong evidences of the specificity of the phenotype observed.

The most distinct morphological phenotype in *cdkn2b* Mo morphants are the turned tails and the curly-down body axis, resembling a phenotype observed in zebrafish with morpholino knockdown of *sox9a and sox9b*[74], *pnpla6*[75], *PINK1*[76] and *Huntingtin*[77].

The knowkdown of *sox9a and sox9b* show embryos with curly-down body axis and turned tail. The authors believed this phenotype to be the loss of expression of the genes in the notochord at about 20hpf [74]. In all the time-points studied we didn´t find expression of the *cdkn2b* in the notochord, but to explore the hypothesis that the phenotype were the result

of the gene expression in the notochord in early stages of development it would necessary to investigate the expression of our protein in early stages of development.

It has been reported that when knocking down *pnpla6*, *PINK1* or *Huntingtin* with morpholinos the embryos presented not only a phenotype similar to ours, but also changes in the brain of the fish. This is due to the relationship between these proteins and neurodegenerative diseases. *Huntingtin,* in particular, besides presenting a phenotype identical to ours (curly-down body axis and turned tail), also shows similarities in mRNA expression of the gene at 48hpf. The authors propose that abnormalities in tail development may be a common feature of zebrafish with deficiency in genes involved in neural development [77].

CDKN2B is usually associated to Alzheimer's disease, due to its increase in brain cells from patients suffering from this disease [79]. *cdkn2b* Mo morphants also presented some neural death that could lead us to a possible relation between *cdkn2b* and neural development. Nonetheless, the neural death wasn't always present in the embryos with turned tails and curly-down body axis and the effects disappear when co-injecting p53 Mo, leading to the conclusion that the neural death observed is a side effect of the morpholino.

In summary, the pattern of expression of *cdkn2b* mRNA and morphants with phenotypes similar to ours existing in the literature led us to hypothesize that the turned tail and curly-down body axis phenotype could be due to changes in expression of *cdkn2b* in the brain of the fish that may not result in a phenotype in the brain. However, to test this hypothesis more studies would be needed.

Aside from the turned tail and curly-down body axis phenotype, and based on the expression pattern of our protein, a phenotype in the epidermis of the fish (due to lack of expression after the knockdown) could be expected. However, the loss of *cdkn2b* expression in the epidermis did not cause a phenotype. Since, in mammalians, members of the INK4 family have redundant functions regulating cell cycle [12], the absence of phenotype could be explained by the existence of proteins with redundant functions to *cdkn2b* (like *cdkn2a*).

Nevertheless, we want to point out that our first aim of characterizing, for the first time, *cdkn2b* expression during zebrafish early development was successfully accomplished.

Regarding the possible relationship between *cdkn2b* and blood vessel formation, we did a knockdown in *fli1a:EGFP* zebrafish, a transgenic that has the blood vessels marked with GFP [50]. This permitted us to analyze the vessels of the fish in detail at the chosen time-points.

At 24hpf, knocking down of *cdkn2b* promoted the deformation of the caudal vein and at later stages (48hpf and 72hpf), conducted to tails with problems on the intersegmental

vessels (Se), the caudal vein and the caudal artery (CA). However, the effect on the Se and CA are possibly the result of morpholino off-target effects, like was observed in embryos under less morpholino neural death effect (co-injected with p53 Mo).

Overall, knocking down of *cdkn2b* seems to be affecting the morphology of the caudal vein of the fish. Nevertheless, it remains the question whether if the cv phenotypes are a consequence of a deformed tail or if *cdkn2b* is affecting directly the vessels formation at the tail and this has consequences at the correct blood supply and subsequent development of the tail of the fish. Future studies are needed to clarify this subject.

In conclusion, in the present work, we have shown the importance of this gene in the correct formation of the fish, and regarding blood vessels of the fish, complementary studies are needed to understand the direct relation between *cdkn2b* and vessels/tail formation.

Chapter 7: **Future Perspectives**

In order to better understand the role of cdkn2b during zebrafish development, and to answer some questions that aroused from the present work, there are some experiments we need to do:

- To clarify the specific localization of *cdkn2b* mRNA expression we need to do *in situ* hybridization in sections of the embryos (to analyze the expression in the cephalic region and the vessels of the fish).
- To see if the phenotype observed is due to the expression of *cdkn2b* at early time-points to the ones studied, we need to characterize expression of mRNA and protein in early time-points.
- We need to characterize *cdkn2a* and its knockdown phenotype to understand if its presence can explain the lack of epidermal phenotype caused by *cdkn2b* knockdown. This should be accompanied by co-injection of morpholinos against both genes.
- To analyze in more detail the blood vessel phenotype in zebrafish embryos we can use Definiens Developer and Definiens Architect software.

Bibliography

[1] G. J. E. Rinkel, M. Djibuti, A. Algra, e J. van Gijn, «Prevalence and Risk of Rupture of Intracranial Aneurysms A Systematic Review», *Stroke*, vol. 29, n. 1, pp. 251-256, Jan 1998.

[2] A. Helgadottir, G. Thorleifsson, K. P. Magnusson, S. Grétarsdottir, V. Steinthorsdottir, A. Manolescu, G. T. Jones, G. J. E. Rinkel, J. D. Blankensteijn, A. Ronkainen, J. E. Jääskeläinen, Y. Kyo, G. M. Lenk, N. Sakalihasan, K. Kostulas, A. Gottsäter, A. Flex, H. Stefansson, T. Hansen, G. Andersen, S. Weinsheimer, K. Borch-Johnsen, T. Jorgensen, S. H. Shah, A. A. Quyyumi, C. B. Granger, M. P. Reilly, H. Austin, A. I. Levey, V. Vaccarino, E. Palsdottir, G. B. Walters, T. Jonsdottir, S. Snorradottir, D. Magnusdottir, G. Gudmundsson, R. E. Ferrell, S. Sveinbjornsdottir, J. Hernesniemi, M. Niemelä, R. Limet, K. Andersen, G. Sigurdsson, R. Benediktsson, E. L. G. Verhoeven, J. A. W. Teijink, D. E. Grobbee, D. J. Rader, D. A. Collier, O. Pedersen, R. Pola, J. Hillert, B. Lindblad, E. M. Valdimarsson, H. B. Magnadottir, C. Wijmenga, G. Tromp, A. F. Baas, Y. M. Ruigrok, A. M. van Rij, H. Kuivaniemi, J. T. Powell, S. E. Matthiasson, J. R. Gulcher, G. Thorgeirsson, A. Kong, U. Thorsteinsdottir, e K. Stefansson, «The same sequence variant on 9p21 associates with myocardial infarction, abdominal aortic aneurysm and intracranial aneurysm», *Nat. Genet.*, vol. 40, n. 2, pp. 217-224, Fev 2008.

[3] H. Hashikata, W. Liu, K. Inoue, Y. Mineharu, S. Yamada, S. Nanayakkara, N. Matsuura, T. Hitomi, Y. Takagi, N. Hashimoto, S. Miyamoto, e A. Koizumi, «Confirmation of an Association of Single-Nucleotide Polymorphism rs1333040 on 9p21 With Familial and Sporadic Intracranial Aneurysms in Japanese Patients», *Stroke*, vol. 41, n. 6, pp. 1138-1144, Jan 2010.

[4] B. G. Kral, R. A. Mathias, B. Suktitipat, I. Ruczinski, D. Vaidya, L. R. Yanek, A. A. Quyyumi, R. S. Patel, A. M. Zafari, V. Vaccarino, E. R. Hauser, W. E. Kraus, L. C. Becker, e D. M. Becker, «A common variant in the CDKN2B gene on chromosome 9p21 protects against coronary artery disease in Americans of African ancestry», *Journal of Human Genetics*, vol. 56, n. 3, pp. 224-229, Jan 2011.

[5] J. G. Smith, O. Melander, H. Lövkvist, B. Hedblad, G. Engström, P. Nilsson, J. Carlson, G. Berglund, B. Norrving, e A. Lindgren, «Common Genetic Variants on Chromosome 9p21 Confers Risk of Ischemic StrokeCLINICAL PERSPECTIVE A Large-Scale Genetic Association Study», *Circ Cardiovasc Genet*, vol. 2, n. 2, pp. 159-164, Jan 2009.

[6] E. T. Cánepa, M. E. Scassa, J. M. Ceruti, M. C. Marazita, A. L. Carcagno, P. F. Sirkin, e M. F. Ogara, «INK4 proteins, a family of mammalian CDK inhibitors with novel biological functions», *IUBMB Life*, vol. 59, n. 7, pp. 419–426, 2007.

[7] E. Chen e S. C. Ekker, «Zebrafish as a genomics research model», *Current Pharmaceutical Biotechnology*, vol. 5, n. 5, pp. 409–413, 2004.

[8] K. Dooley e L. I. Zon, «Zebrafish: a model system for the study of human disease», *Current opinion in genetics & development*, vol. 10, n. 3, pp. 252–256, 2000.

[9] T. Piotrowski, D. Ahn, T. F. Schilling, S. Nair, I. Ruvinsky, R. Geisler, G.-J. Rauch, P. Haffter, L. I. Zon, Y. Zhou, H. Foott, I. B. Dawid, e R. K. Ho, «The zebrafish van gogh mutation disrupts tbx1, which is involved in the DiGeorge deletion syndrome in humans», *Development*, vol. 130, n. 20, pp. 5043-5052, Out 2003.

[10] N. D. Lawson e B. M. Weinstein, «In vivo imaging of embryonic vascular development using transgenic zebrafish», *Dev. Biol.*, vol. 248, n. 2, pp. 307-318, Ago 2002.

[11] W. Y. Kim e N. E. Sharpless, «The Regulation of INK4/ARF in Cancer and Aging», *Cell*, vol. 127, n. 2, pp. 265-275, Out 2006.

[12] Martine F Roussel, «The INK4 family of cell cycle inhibitors in cancer», *, Published online: 20 September 1999; | doi:10.1038/sj.onc.1202998*, vol. 18, n. 38, Set 1999.

[13] M. Malumbres e M. Barbacid, «Milestones in cell division : To cycle or not to cycle: a critical decision in cancer», *Nature Reviews Cancer*, vol. 1, n. 3, pp. 222-231, Dez 2001.

[14] T. Arendt, M. Holzer, e U. Gärtner, «Neuronal expression of cycline dependent kinase inhibitors of the INK4 family in Alzheimer's disease», *Journal of Neural Transmission*, vol. 105, n. 8, pp. 949-960, 1998.

[15] M. Serrano, G. J. Hannon, e D. Beach, «A new regulatory motif in cell-cycle control causing specific inhibition of cyclin D/CDK4», *Nature*, vol. 366, n. 6456, pp. 704-707, Dez 1993.

[16] G. J. Hannon e D. Beach, «p15INK4B is a potential effector of TGF-beta-induced cell cycle arrest», *Nature*, vol. 371, n. 6494, pp. 257-261, Set 1994.

[17] K. L. Guan, C. W. Jenkins, Y. Li, M. A. Nichols, X. Wu, C. L. O'Keefe, A. G. Matera, e Y. Xiong, «Growth suppression by p18, a p16INK4/MTS1- and p14INK4B/MTS2-related CDK6 inhibitor, correlates with wild-type pRb function.», *Genes Dev.*, vol. 8, n. 24, pp. 2939-2952, Dez 1994.

[18] H. Hirai, M. F. Roussel, J. Y. Kato, R. A. Ashmun, e C. J. Sherr, «Novel INK4 proteins, p19 and p18, are specific inhibitors of the cyclin D-dependent kinases CDK4 and CDK6.», *Mol Cell Biol*, vol. 15, n. 5, pp. 2672-2681, Mai 1995.

[19] M. Esteller, P. G. Corn, S. B. Baylin, e J. G. Herman, «A Gene Hypermethylation Profile of Human Cancer», *Cancer Res*, vol. 61, n. 8, pp. 3225-3229, Abr 2001.

[20] J.-M. Li, P. P. Hu, X. Shen, Y. Yu, e X.-F. Wang, «E2F4-RB and E2F4-p107 complexes suppress gene expression by transforming growth factor β through E2F binding sites», *Proc Natl Acad Sci U S A*, vol. 94, n. 10, pp. 4948-4953, Mai 1997.

[21] I. Reynisdóttir, K. Polyak, A. Iavarone, e J. Massagué, «Kip/Cip and Ink4 Cdk inhibitors cooperate to induce cell cycle arrest in response to TGF-beta.», *Genes Dev.*, vol. 9, n. 15, pp. 1831-1845, Jan 1995.

[22] K. Musunuru, W. S. Post, W. Herzog, H. Shen, J. R. O'Connell, P. F. McArdle, K. A. Ryan, Q. Gibson, Y.-C. Cheng, E. Clearfield, A. D. Johnson, G. Tofler, Q. Yang, C. J. O'Donnell, D. M. Becker, L. R. Yanek, L. C. Becker, N. Faraday, L. F. Bielak, P. A. Peyser, A. R. Shuldiner, e B. D. Mitchell, «Association of SNPs on Chromosome 9p21.3 with Platelet Reactivity: A Potential Mechanism for Increased Vascular Disease», *Circ Cardiovasc Genet*, vol. 3, n. 5, pp. 445-453, Out 2010.

[23] J. B. Kim, A. Deluna, I. N. Mungrue, C. Vu, D. Pouldar, M. Civelek, L. Orozco, J. Wu, X. Wang, S. Charugundla, L. W. Castellani, M. Rusek, H. Jakobowski, e A. J. Lusis, «Effect of 9p21.3 coronary artery disease locus neighboring genes on atherosclerosis in mice», *Circulation*, vol. 126, n. 15, pp. 1896-1906, Out 2012.

[24] A. Kamb, N. A. Gruis, J. Weaver-Feldhaus, Q. Liu, K. Harshman, S. V. Tavtigian, E. Stockert, R. S. Day 3rd, B. E. Johnson, e M. H. Skolnick, «A cell cycle regulator potentially involved in genesis of many tumor types», *Science*, vol. 264, n. 5157, pp. 436-440, Abr 1994.

[25] N. Popov e J. Gil, «Epigenetic regulation of the INK4b-ARF-INK4a locus: In sickness and in health», *Epigenetics*, vol. 5, n. 8, pp. 685-690, Nov 2010.

[26] J. Gil e G. Peters, «Regulation of the INK4b–ARF–INK4a tumour suppressor locus: all for one or one for all», *Nature Reviews Molecular Cell Biology*, vol. 7, n. 9, pp. 667-677, Jan 2006.

[27] J. G. Mike Fried, «One INK4 gene and no ARF at the Fugu equivalent of the human INK4A/ARF/INK4B tumour suppressor locus», *, Published online: 02 November 2001; | doi:10.1038/sj.onc.1204933*, vol. 20, n. 50, Nov 2001.

[28] A. Congrains, K. Kamide, R. Oguro, O. Yasuda, K. Miyata, E. Yamamoto, T. Kawai, H. Kusunoki, H. Yamamoto, Y. Takeya, K. Yamamoto, M. Onishi, K. Sugimoto, T. Katsuya, N. Awata, K. Ikebe, Y. Gondo, Y. Oike, M. Ohishi, e H. Rakugi, «Genetic variants at the 9p21 locus contribute to atherosclerosis through modulation of ANRIL and CDKN2A/B», *Atherosclerosis*, vol. 220, n. 2, pp. 449-455, Fev 2012.

[29] Y. Kotake, T. Nakagawa, K. Kitagawa, S. Suzuki, N. Liu, M. Kitagawa, e Y. Xiong, «Long non-coding RNA ANRIL is required for the PRC2 recruitment to and silencing of p15INK4B tumor suppressor gene», *Oncogene*, vol. 30, n. 16, pp. 1956-1962, Dez 2010.

[30] H. M. Broadbent, J. F. Peden, S. Lorkowski, A. Goel, H. Ongen, F. Green, R. Clarke, R. Collins, M. G. Franzosi, G. Tognoni, U. Seedorf, S. Rust, P. Eriksson, A. Hamsten, M. Farrall, H. Watkins, e for the PROCARDIS consortium, «Susceptibility to coronary artery disease and diabetes is encoded by distinct, tightly linked SNPs in the ANRIL locus on chromosome 9p», *Human Molecular Genetics*, vol. 17, n. 6, pp. 806-814, Nov 2007.

[31] A. Matheu, C. Pantoja, A. Efeyan, L. M. Criado, J. Martín-Caballero, J. M. Flores, P. Klatt, e M. Serrano, «Increased gene dosage of Ink4a/Arf results in cancer resistance and normal aging», *Genes Dev.*, vol. 18, n. 22, pp. 2736-2746, Nov 2004.

[32] H. Ding, Y. Xu, X. Wang, Q. Wang, L. Zhang, Y. Tu, J. Yan, W. Wang, R. Hui, C.-Y. Wang, e D. W. Wang, «9p21 is a Shared Susceptibility Locus Strongly for Coronary Artery Disease and Weakly for Ischemic Stroke in Chinese Han PopulationCLINICAL PERSPECTIVE», *Circ Cardiovasc Genet*, vol. 2, n. 4, pp. 338-346, Jan 2009.

[33] O. Jarinova, A. F. R. Stewart, R. Roberts, G. Wells, P. Lau, T. Naing, C. Buerki, B. W. McLean, R. C. Cook, J. S. Parker, e R. McPherson, «Functional Analysis of the Chromosome 9p21.3 Coronary

Artery Disease Risk Locus», *Arteriosclerosis, Thrombosis, and Vascular Biology*, vol. 29, n. 10, pp. 1671-1677, Jul 2009.

[34] K. Bilguvar, K. Yasuno, M. Niemelä, Y. M. Ruigrok, M. von und zu Fraunberg, C. M. van Duijn, L. H. van den Berg, S. Mane, C. E. Mason, M. Choi, E. Gaál, Y. Bayri, L. Kolb, Z. Arlier, S. Ravuri, A. Ronkainen, A. Tajima, A. Laakso, A. Hata, H. Kasuya, T. Koivisto, J. Rinne, J. Öhman, M. M. B. Breteler, C. Wijmenga, M. W. State, G. J. E. Rinkel, J. Hernesniemi, J. E. Jääskeläinen, A. Palotie, I. Inoue, R. P. Lifton, e M. Günel, «Susceptibility loci for intracranial aneurysm in European and Japanese populations», *Nat Genet*, vol. 40, n. 12, pp. 1472-1477, Dez 2008.

[35] I. Buysschaert, K. F. Carruthers, D. R. Dunbar, G. Peuteman, E. Rietzschel, A. Belmans, A. Hedley, T. De Meyer, A. Budaj, F. Van de Werf, D. Lambrechts, e K. A. A. Fox, «A variant at chromosome 9p21 is associated with recurrent myocardial infarction and cardiac death after acute coronary syndrome: The GRACE Genetics Study», *Eur Heart J*, vol. 31, n. 9, pp. 1132-1141, Mai 2010.

[36] G.-Q. Shen, S. Rao, N. Martinelli, L. Li, O. Olivieri, R. Corrocher, K. G. Abdullah, S. L. Hazen, J. Smith, J. Barnard, E. F. Plow, D. Girelli, e Q. K. Wang, «Association between four SNPs on chromosome 9p21 and myocardial infarction is replicated in an Italian population», *Journal of Human Genetics*, vol. 53, n. 2, pp. 144-150, Jan 2008.

[37] S. Züchner, J. R. Gilbert, E. R. Martin, C. R. Leon-Guerrero, P.-T. Xu, C. Browning, P. G. Bronson, P. Whitehead, D. E. Schmechel, J. L. Haines, e M. A. Pericak-Vance, «Linkage and association study of late-onset Alzheimer disease families linked to 9p21.3», *Ann Hum Genet*, vol. 72, n. Pt 6, p. 725, Nov 2008.

[38] N. J. Samani, J. Erdmann, A. S. Hall, C. Hengstenberg, M. Mangino, B. Mayer, R. J. Dixon, T. Meitinger, P. Braund, H.-E. Wichmann, J. H. Barrett, I. R. König, S. E. Stevens, S. Szymczak, D.-A. Tregouet, M. M. Iles, F. Pahlke, H. Pollard, W. Lieb, F. Cambien, M. Fischer, W. Ouwehand, S. Blankenberg, A. J. Balmforth, A. Baessler, S. G. Ball, T. M. Strom, I. Brænne, C. Gieger, P. Deloukas, M. D. Tobin, A. Ziegler, J. R. Thompson, e H. Schunkert, «Genomewide Association Analysis of Coronary Artery Disease», *N Engl J Med*, vol. 357, n. 5, pp. 443-453, Ago 2007.

[39] Kathiresan S, Voight BF, Purcell S, Musunuru K, Ardissino D, Mannucci PM, Anand S, Engert JC, Samani NJ, Schunkert H, Erdmann J, Reilly MP, Rader DJ, Morgan T, Spertus JA, Stoll M, Girelli D, McKeown PP, Patterson CC, Siscovick DS, O'Donnell CJ, Elosua R, Peltonen L, Salomaa V, Schwartz SM, Melander O, Altshuler D, Ardissino D, Merlini PA, Berzuini C, Bernardinelli L, Peyvandi F, Tubaro M, Celli P, Ferrario M, Fetiveau R, Marziliano N, Casari G, Galli M, Ribichini F, Rossi M, Bernardi F, Zonzin P, Piazza A, Mannucci PM, Schwartz SM, Siscovick DS, Yee J, Friedlander Y, Elosua R, Marrugat J, Lucas G, Subirana I, Sala J, Ramos R, Kathiresan S, Meigs JB, Williams G, Nathan DM, MacRae CA, O'Donnell CJ, Salomaa V, Havulinna AS, Peltonen L, Melander O, Berglund G, Voight BF, Kathiresan S, Hirschhorn JN, Asselta R, Duga S, Spreafico M, Musunuru K, Daly MJ, Purcell S, Voight BF, Purcell S, Nemesh J, Korn JM, McCarroll SA, Schwartz SM, Yee J, Kathiresan S, Lucas G, Subirana I, Elosua R, Surti A, Guiducci C, Gianniny L, Mirel D, Parkin M, Burtt N, Gabriel SB, Samani NJ, Thompson JR, Braund PS, Wright BJ, Balmforth AJ, Ball SG, Hall AS; Wellcome Trust Case Control Consortium, Schunkert H, Erdmann J, Linsel-Nitschke P, Lieb W, Ziegler A, König I, Hengstenberg C, Fischer M, Stark K, Grosshennig A, Preuss M, Wichmann HE, Schreiber S, Schunkert H, Samani NJ, Erdmann J, Ouwehand W, Hengstenberg C, Deloukas P, Scholz M, Cambien F, Reilly MP, Li M, Chen Z, Wilensky R, Matthai W, Qasim A, Hakonarson HH, Devaney J, Burnett MS, Pichard AD, Kent KM, Satler L, Lindsay JM, Waksman R, Knouff CW, Waterworth DM, Walker MC, Mooser V, Epstein SE, Rader DJ, Scheffold T, Berger K, Stoll M, Huge A, Girelli D, Martinelli N, Olivieri O, Corrocher R, Morgan T, Spertus JA, McKeown P, Patterson CC, Schunkert H, Erdmann E, Linsel-Nitschke P, Lieb W, Ziegler A, König IR, Hengstenberg C, Fischer M, Stark K, Grosshennig A, Preuss M, Wichmann HE, Schreiber S, Hólm H, Thorleifsson G, Thorsteinsdottir U, Stefansson K, Engert JC, Do R, Xie C, Anand S, Kathiresan S, Ardissino D, Mannucci PM, Siscovick D, O'Donnell CJ, Samani NJ, Melander O, Elosua R, Peltonen L, Salomaa V, Schwartz SM, Altshuler D., «Genome-wide association of early-onset myocardial infarction with common single nucleotide polymorphisms, common copy number variants, and rare copy number variants», *Nat Genet*, vol. 41, n. 3, pp. 334-341, Mar 2009.

[40] K. Hinohara, T. Nakajima, M. Takahashi, S. Hohda, T. Sasaoka, K. Nakahara, K. Chida, M. Sawabe, T. Arimura, A. Sato, B.-S. Lee, J. Ban, M. Yasunami, J.-E. Park, T. Izumi, e A. Kimura, «Replication of the association between a chromosome 9p21 polymorphism and coronary artery disease in Japanese and Korean populations», *Journal of Human Genetics*, vol. 53, n. 4, pp. 357-359, Jan 2008.

[41] T. L. Assimes, J. W. Knowles, A. Basu, C. Iribarren, A. Southwick, H. Tang, D. Absher, J. Li, J. M. Fair, G. D. Rubin, S. Sidney, S. P. Fortmann, A. S. Go, M. A. Hlatky, R. M. Myers, N. Risch, e T. Quertermous, «Susceptibility locus for clinical and subclinical coronary artery disease at chromosome 9p21 in the multi-ethnic ADVANCE study», *Hum Mol Genet*, vol. 17, n. 15, pp. 2320-2328, Ago 2008.

[42] B. Krischek e I. Inoue, «The genetics of intracranial aneurysms», *Journal of Human Genetics*, vol. 51, n. 7, pp. 587-594, 2006.

[43] Y. M. Ruigrok, G. J. Rinkel, e C. Wijmenga, «Genetics of intracranial aneurysms», *The Lancet Neurology*, vol. 4, n. 3, pp. 179-189, Mar 2005.

[44] J. A. Jones, J. R. Barbour, R. E. Stroud, S. Bouges, S. L. Stephens, F. G. Spinale, e J. S. Ikonomidis, «Altered Transforming Growth Factor-beta Signaling in a Murine Model of Thoracic Aortic Aneurysm», *J Vasc Res*, vol. 45, n. 6, pp. 457-468, 2008.

[45] «2000 Wixon - Danio rerio, the zebrafish.pdf». .

[46] C. B. Kimmel, W. W. Ballard, S. R. Kimmel, B. Ullmann, e T. F. Schilling, «Stages of embryonic development of the zebrafish», *Developmental dynamics*, vol. 203, n. 3, pp. 253–310, 1995.

[47] B. J. Holden, D. G. Bratt, e T. J. A. Chico, «Molecular control of vascular development in the zebrafish», *Birth Defects Research Part C: Embryo Today: Reviews*, vol. 93, n. 2, pp. 134-140, Jun 2011.

[48] S. Isogai, M. Horiguchi, e B. M. Weinstein, «The Vascular Anatomy of the Developing Zebrafish: An Atlas of Embryonic and Early Larval Development», *Developmental Biology*, vol. 230, n. 2, pp. 278-301, Fev 2001.

[49] B. L. Roman e B. M. Weinstein, «Building the vertebrate vasculature: research is going swimmingly», *BioEssays*, vol. 22, n. 10, pp. 882–893, 2000.

[50] N. D. Lawson e B. M. Weinstein, «In Vivo Imaging of Embryonic Vascular Development Using Transgenic Zebrafish», *Developmental Biology*, vol. 248, n. 2, pp. 307-318, Ago 2002.

[51] A. Padmanabhan, J.-S. Lee, F. A. Ismat, M. M. Lu, N. D. Lawson, J. P. Kanki, A. T. Look, e J. A. Epstein, «Cardiac and vascular functions of the zebrafish orthologues of the type I neurofibromatosis gene NFI», *PNAS*, vol. 106, n. 52, pp. 22305-22310, Dez 2009.

[52] S. Isogai, M. Horiguchi, e B. M. Weinstein, «The Vascular Anatomy of the Developing Zebrafish: An Atlas of Embryonic and Early Larval Development», *Developmental Biology*, vol. 230, n. 2, pp. 278-301, Fev 2001.

[53] W.-J. Chang e P.-P. Hwang, «Development of zebrafish epidermis», *Birth Defects Research Part C: Embryo Today: Reviews*, vol. 93, n. 3, pp. 205–214, 2011.

[54] Q. Li, M. Frank, C. Thisse, B. Thisse, e J. Uitto, «Zebrafish: A Model System to Study Heritable Skin Diseases», *J Invest Dermatol*, vol. 131, n. 3, pp. 565-571, Mar 2011.

[55] D. Le Guellec, G. Morvan-Dubois, e J.-Y. Sire, «Skin development in bony fish with particular emphasis on collagen deposition in the dermis of the zebrafish (Danio rerio)», *Int. J. Dev. Biol.*, vol. 48, n. 2-3, pp. 217-231, 2004.

[56] W.-J. Chang e P.-P. Hwang, «Development of zebrafish epidermis», *Birth Defects Research Part C: Embryo Today: Reviews*, vol. 93, n. 3, pp. 205–214, 2011.

[57] C. J. Ceol, Y. Houvras, R. M. White, e L. I. Zon, «Melanoma Biology and the Promise of Zebrafish», *Zebrafish*, vol. 5, n. 4, pp. 247-255, Dez 2008.

[58] M. J. Redd, G. Kelly, G. Dunn, M. Way, e P. Martin, «Imaging macrophage chemotaxis in vivo: studies of microtubule function in zebrafish wound inflammation», *Cell Motil. Cytoskeleton*, vol. 63, n. 7, pp. 415-422, Jul 2006.

[59] S. A. Renshaw, C. A. Loynes, D. M. I. Trushell, S. Elworthy, P. W. Ingham, e M. K. B. Whyte, «A transgenic zebrafish model of neutrophilic inflammation», *Blood*, vol. 108, n. 13, pp. 3976-3978, Dez 2006.

[60] R. T. Peterson, S. Y. Shaw, T. A. Peterson, D. J. Milan, T. P. Zhong, S. L. Schreiber, C. A. MacRae, e M. C. Fishman, «Chemical suppression of a genetic mutation in a zebrafish model of aortic coarctation», *Nat. Biotechnol.*, vol. 22, n. 5, pp. 595-599, Mai 2004.

[61] B. R. Bill, A. M. Petzold, K. J. Clark, L. A. Schimmenti, e S. C. Ekker, «A primer for morpholino use in zebrafish», *Zebrafish*, vol. 6, n. 1, pp. 69–77, 2009.

[62] S. C. Ekker, «Morphants: a new systematic vertebrate functional genomics approach», *Yeast*, vol. 17, n. 4, pp. 302–306, 2000.

[63] J. S. Eisen e J. C. Smith, «Controlling morpholino experiments: don't stop making antisense», *Development*, vol. 135, n. 10, pp. 1735-1743, Abr 2008.

[64] A. N. Stephen C. Ekker, «Effective targeted gene “knockdown” in zebrafish», vol. 26, pp. 216-220, Out 2000.
[65] V. M. Bedell, S. E. Westcot, e S. C. Ekker, «Lessons from morpholino-based screening in zebrafish», *Briefings in Functional Genomics*, vol. 10, n. 4, pp. 181-188, Jul 2011.
[66] S. C. Ekker e J. D. Larson, «Morphant technology in model developmental systems», *Genesis*, vol. 30, n. 3, pp. 89–93, 2001.
[67] D. R. Corey, J. M. Abrams, e others, «Morpholino antisense oligonucleotides: tools for investigating vertebrate development», *Genome Biol*, vol. 2, n. 5, p. 1015, 2001.
[68] J. Heasman, «Morpholino Oligos: Making Sense of Antisense?», *Developmental Biology*, vol. 243, n. 2, pp. 209-214, Mar 2002.
[69] M. E. Robu, J. D. Larson, A. Nasevicius, S. Beiraghi, C. Brenner, S. A. Farber, e S. C. Ekker, «p53 activation by knockdown technologies», *PLoS genetics*, vol. 3, n. 5, p. e78, 2007.
[70] C. Thisse e B. Thisse, «High-resolution in situ hybridization to whole-mount zebrafish embryos», *Nat Protoc*, vol. 3, n. 1, pp. 59-69, 2008.
[71] P. Chapouton, P. Skupien, B. Hesl, M. Coolen, J. C. Moore, R. Madelaine, E. Kremmer, T. Faus-Kessler, P. Blader, N. D. Lawson, e L. Bally-Cuif, «Notch Activity Levels Control the Balance between Quiescence and Recruitment of Adult Neural Stem Cells», *J. Neurosci.*, vol. 30, n. 23, pp. 7961-7974, Set 2010.
[72] R. M. Alani, J. Hasskarl, e K. Münger*, «Alterations in cyclin-dependent kinase 2 function during differentiation of primary human keratinocytes», *Molecular Carcinogenesis*, vol. 23, n. 4, pp. 226–233, 1998.
[73] «Defects in TGFβ signaling overcome senescence of mouse keratinocytes expressing v-rasHa», , *Published online: 29 March 2000; | doi:10.1038/sj.onc.1203471*, vol. 19, n. 13, Mar 2000.
[74] Y.-L. Yan, J. Willoughby, D. Liu, J. G. Crump, C. Wilson, C. T. Miller, A. Singer, C. Kimmel, M. Westerfield, e J. H. Postlethwait, «A pair of Sox: distinct and overlapping functions of zebrafish sox9 co-orthologs in craniofacial and pectoral fin development», *Development*, vol. 132, n. 5, pp. 1069-1083, Jan 2005.
[75] Y. Song, M. Wang, F. Mao, M. Shao, B. Zhao, Z. Song, C. Shao, e Y. Gong, «Knockdown of pnpla6 protein results in motor neuron defects in zebrafish», *Dis. Model. Mech.*, Set 2012.
[76] O. Anichtchik, H. Diekmann, A. Fleming, A. Roach, P. Goldsmith, e D. C. Rubinsztein, «Loss of PINK1 Function Affects Development and Results in Neurodegeneration in Zebrafish», *J. Neurosci.*, vol. 28, n. 33, pp. 8199-8207, Ago 2008.
[77] A. L. Lumsden, T. L. Henshall, S. Dayan, M. T. Lardelli, e R. I. Richards, «Huntingtin-deficient zebrafish exhibit defects in iron utilization and development», *Hum. Mol. Genet.*, vol. 16, n. 16, pp. 1905-1920, Ago 2007.
[78] Y. Song, M. Wang, F. Mao, M. Shao, B. Zhao, Z. Song, C. Shao, e Y. Gong, «Knockdown of pnpla6 protein results in motor neuron defects in zebrafish», *Dis. Model. Mech.*, Set 2012.
[79] F. Cortini, C. Fenoglio, E. Venturelli, C. Villa, F. Clerici, M. Serpente, C. Cantoni, G. Fumagalli, C. Mariani, N. Bresolin, E. Scarpini, e D. Galimberti, «Cell-dependent kinase inhibitor <i>2A</i> and <i>2B</i> genetic variability in patients with Alzheimer’s disease», *Journal of Neurology*, vol. 258, n. 4, pp. 704-705, 2011.